Geochemical and metallogenic relations in volcanic rocks of the southern Slave Province: implications for late Neoarchean tectonics

A.M. Goodwin, M.B. Lambert, and O. Ujike

Abstract: Late Neoarchean volcanic belts in the southern Slave Province include (1) in the east, the Cameron River – Beaulieu River belts, which are characterized by stratigraphically thin, flow-rich, classic calc-alkaline, arc-type sequences with accompanying syngenetic volcanogenic massive sulphide deposits; and (2) in the west, the Yellowknife belt, which is characterized by stratigraphically thick, structurally complex, pyroclastic-rich, adakitic, back-arc basin-type sequences, with accompanying epigenetic lode-gold deposits. The volcanic belt association bears persuasive chemical evidence of subduction-initiated magma generation. However, the greenstone belts, together with coeval matching patterned belts in Superior Province of the southern Canadian Shield, bear equally persuasive evidence of prevailing autochthonous–parautochthonous relations with respect to component stratigraphic parts and to older gneissic basement. The eastern and western volcanic belts in question are petrogenetically ascribed to a "westerly inclined" (present geography) subduction zone(s) that produced shallower (east) to deeper (west), slab-initiated, mantle wedge-generated, parent magmas. This early stage microplate tectonic process involved modest mantle subduction depths, small tectonic plates, and small sialic cratons. In the larger context of Earth's progressively cooling, hence subduction-deepening mantle, this late Neoarchean greenstone belt development (2.73–2.66 Ga) merged with the massive end-Archean tonalite–trondhjemite–granodiorite–granite (TTGG) "bloom" (2.65–2.55 Ga), resulting in greatly enhanced craton stability. Successive subduction-deepening, plate-craton-enlarging stages, with appropriate metallotectonic response across succeeding Proterozoic time and beyond, led to modern-mode plate tectonics.

Résumé : Les ceintures volcaniques dans le sud de la Province des Esclaves comprennent (1) à l'est, les ceintures des rivières Cameron et Beaulieu, lesquelles sont caractérisées par des séquences de type arc, classiques calco-alcalines, minces et riches en écoulements, avec des gisements de sulfures massifs volcanogènes syngénétiques qui les accompagnent et (2) à l'ouest, la ceinture de Yellowknife, laquelle est caractérisée par des séquences à structure complexe de type bassin d'arrière-arc, adakitiques, riches en roches pyroclastiques et accompagnées de gisements d'or filonien épigénétiques. L'association des ceintures volcaniques comporte des évidences chimiques de génération de magmas initiée par de la subduction. Toutefois, les ceintures de roches vertes, ainsi que des ceintures contemporaines, à patrons assortis, dans la Province du Supérieur dans le sud du Bouclier canadien, comportent des éléments probants, aussi convaincants, de relations autochtones–parautochtones prédominantes par rapport aux composantes stratigraphiques et au socle gneissique plus ancien. Les ceintures volcaniques de l'est et de l'ouest ont été assignées de manière pétrogénétique à une ou des zones de subduction « inclinée vers l'ouest » (géographie actuelle) qui ont produit des magmas parents moins profonds (à l'est) à plus profonds (à l'ouest); ces magmas proviendraient de dalles et de coins du manteau. Ce processus de tectonique de micro-plaques, à un stade précoce, signifiait des profondeurs modestes de subduction du manteau, de petites plaques tectoniques et de petits cratons sialiques. Dans le contexte plus grand du refroidissement progressif de la Terre, donc d'un manteau s'approfondissant par subduction, le développement de cette ceinture de roches vertes au Néoarchéen tardif (2,73–2,66 Ga) s'est uni avec une « poussée » de tonalite–trondhjémite–granodiorite–granite (TTGG) à la fin de l'Archéen (2,65–2,55 Ga), ce qui a grandement amélioré la stabilité du craton. Des étapes successives de d'approfondissement par subduction, d'agrandissement des plaques-cratons, avec une réponse appropriée de métallotectes, à travers l'époque protérozoïque suivante et plus tardivement encore, a conduit au mode moderne de tectonique des plaques.

[Traduit par la Rédaction]

Received 14 June 2005. Accepted 28 June 2006. Published on the NRC Research Press Web site at http://cjes.nrc.ca on 7 February 2007.

Paper handled by Associate Editor K. Ansdell.

A.M. Goodwin.[1] Department of Geology, Earth Sciences Centre, University of Toronto, 22 Russell Street, Toronto, ON M5S 3B1, Canada.
M.B. Lambert. Geological Survey of Canada, 601 Booth Street, Ottawa, ON K1A 0E8, Canada.
S. Ujike. Department of Earth Sciences, Toyama University, Gofuku 3190, Toyama, 930 8555, Japan.

[1]Corresponding author (e-mail: a.goodwin@rogers.com).

 doi:10.1139/E06-074

Introduction

Cameron River – Beaulieu River (CR–BR) volcanic belts lie 110 km east of the Yellowknife volcanic belt in the southern Slave Province, northern Canadian Shield (Fig. 1). Geochemical–mineral deposit relations in these late Neoarchean volcanic belts provide a distinctive regional metallotectonic pattern; this pattern is matched in coeval greenstone regions of Superior Province, southern Canadian Shield, and elsewhere. This paper presents new data from the CR–BR area and uses data published elsewhere. All cited ages are based on U–Pb dating.

Slave Province

Slave Province contains some 26 comparatively small late Neoarchean (2730–2660 Ma) greenstone belts. The belts typically lie at the margins of marginally younger metaturbidite basins (2680–2660 Ma), of which Yellowknife Supracrustal Basin, which separates CR–BR and Yellowknife belts, ranks amongst the largest (Fig. 1). The pan-Slave metasupracrustal composite, which underlies about half the province, is termed the Yellowknife Supergroup (Henderson 1970, 1985). The remainder of the province is mainly underlain by assorted granitoid rocks, which include both widespread younger Neoarchean plutonic suites and remnant patches of pre-greenstone gneiss–migmatite basement (e.g., Sleepy Dragon and Anton complexes); the basement has been dated at 2.8–4.0 Ga (Bowring and Housh 1995; Isachsen and Bowring 1994). Bleeker et al. (1999*a*) tentatively divided Slave Province basement rocks into northwestern and southwestern complexes. The latter, the Central Slave basement complex, which extends 180 km east of Yellowknife and 340 km north of Great Slave Lake (see Bleeker et al. 1999*a*, fig. 3), comprises heterogeneous dioritic–tonalitic gneisses, migmatite, and mafic dyke swarms, collectively dated at 2.8–3.4 Ga. Bleeker et al. (2000) subsequently proposed that Slave Province gneiss–migmatite basement rocks, in fact, formed a single coherent cratonic nucleus by 2.85 Ga; this nucleus originally extended northwestward into much of the adjoining Paleoproterozoic-designated central Wopmay fold belt.

The unconformably overlying Yellowknife Supergroup (Figs. 1, 2) includes (1) thin (generally <200m) discontinuous Central Slave Cover Group (Bleeker et al. 1999*a*; Ketchum et al. 2004), a (par)authochthonous continental-shelf assemblage composed of highly sheared, basal quartzite–conglomerate banded iron formation (BIF) with local mafic–ultramafic volcanic associates, collectively dated at 2835–2734 Ma (Ketchum et al. 2004); and (2) thick, tholeiitic to calc-alkaline volcanic sequences (e.g., Kam–Banting groups of the Yellowknife belt, and Beaulieu Group of the CR–BR belts (2730–2660 Ma), respectively). The volcanic belts, which have highly strained lower contacts with underlying rocks, are in conformable contact with (3) coeval to marginally younger metasedimentary rocks, notably Burwash metaturbidites (2680–2660 Ma) of the Duncan Lake Group (Bleeker et al. 1999*a*, 1999*b*). Subsequent pan-Slave granitoid plutonism (2630–2580 Ma) includes 2630–2605 Ma tonalite–trondhjemite–granodiorite (TTG) followed by 2600–2580 Ma granites (Davis et al. 1994; Davis and Bleeker 1999). Two accompanying deformations (and) or metamorphisms are dated, respectively, at 2630–2620 Ma (D1/F1) and 2600–2590 Ma (D2 /F2), with resulting regional fold interpretations (Fig. 1) after Davis and Bleeker (1999).

Regionally, Bleeker et al. (1999*a*) proposed a stratigraphic link between coeval Yellowknife and CR–BR volcanic belts, which would lie accordingly on opposing limbs of a regional synclinorium or structural basin. Indeed, rhyolite flows at comparatively high levels in both CR–BR and Yellowknife belts yield identical ages of 2663 Ma (Ketchum et al. 2004). However, the composition of the buried basement beneath the intervening Yellowknife Supracrustal Basin remains largely undetermined.

Lithotectonic models for Slave Province greenstone belts are broadly grouped into allochthonous and (par)authochtonous headings (Ketchum et al. 2004). Thus, Kusky (1990) interpreted the regional greenstones as far-travelled, west-directed, oceanic allochthonous fold and thrust belts with lower mafic and overlying intermediate–felsic volcanic units, respectively, representing ophiolites and superimposed arc magmas. Other workers (Bleeker et al. 1999*a*; Ketchum et al. 2004) favoured eruption–deposition of greenstones onto sialic basement, with maximum horizontal displacements limited to a few tens of kilometres and with the volcanic belts themselves being separated from subjacent basement (e.g., Sleepy Dragon complex) by a regional décollement zone (e.g., Patterson Lake structural complex).

In this regard, Bleeker et al. (1999*b*) reexamined basement-cover relations of the Sleepy Dragon complex in the CR–BR region and confirmed the presence of an extensive, intervening décollement or high-strain zone. They considered (1) the thin Central Slave Cover Group to be autochthonous–parautochthonous upon this basement, (2) the thick overlying Beaulieu tholeiitic basalts (e.g. Cameron River basalts) to be parautochtonous upon it, and (3) the overlying Beaulieu calc-alkaline volcanic sequences (e.g. Webb Lake andesite) to be in turn autochthonous upon the tholeiites. The transport direction along this regional décollement was northeast to southwest, with maximum displacements in the order of 10 to several tens of kilometres. According to dated dyke swarm emplacements, the permissible age range of the décollement-controlling high-strain event is 2734-2687 Ma.

Cameron River – Beaulieu River volcanic belts

Beaulieu Group volcanic belts, with underlying locally exposed Central Slave Cover Group formations, envelope the southern closure of the 20–40 km wide Sleepy Dragon complex (Figs. 1, 2). This U-shaped belt pattern divides naturally into three subareas: (1) Cameron River subarea (belt) in the west, forming the southern extremity of the Cameron River belt, which extends another 45 km north of the map area; (2) Sunset Lake subarea in the east, a southern part of the Beaulieu River belt, which extends another 110 km to the north (Dostal and Corcoran 1998); and (3) Tumpline Lake subarea in the south, which is the presumed southern extension of the Beaulieu River belt. Burwash metasedimentary rocks of the Duncan Lake Group conformably overlie Beaulieu volcanic rocks to the west, south, and partly east. Raquette Lake metasediments, which are further considered later in the text, locally unconformably overlie Cameron River basalts

Fig. 1. General geologic map of southern Slave Province showing location of Yellowknife and Cameron River – Beaulieu River volcanic belts, with main mafic dyke swarms; and subjacent Central Slave Cover Group formations. Boxed area is that of Fig. 2. Inset map shows the location of Slave Province, Yellowknife, and the Cameron River – Beaulieu River map area. After Lambert (1988, figs. 2, 3); Davis and Bleeker (1992, fig. 2); Bleeker et al. (1999*a*, fig. 7).

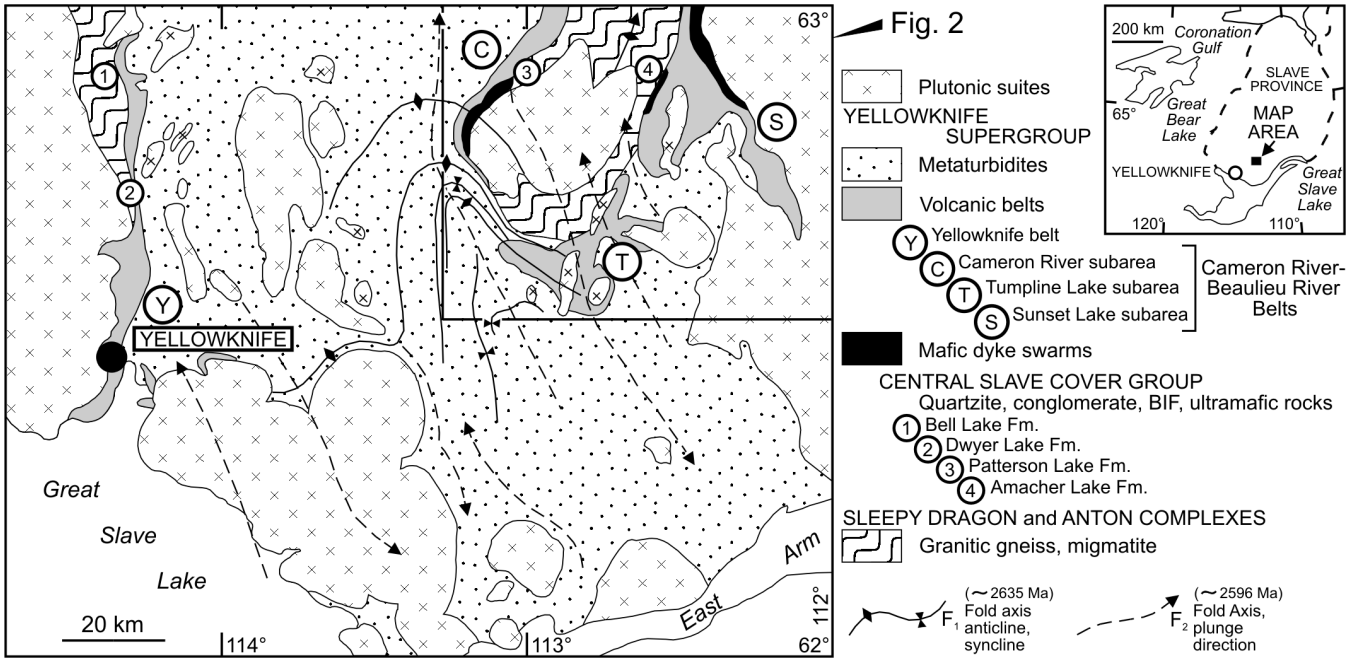

and underlie Burwash metasediments in the 7 km long Upper Ross – Victory lakes interval (Fig. 2). Younger Archean plutonic suites intrude these metasupracrustal rocks and basement gneisses and abound to the east.

Bleeker et al. (1999*a*) demonstrated that the southern closure of the basement complex represents a steeply plunging, second-generation fold axis related to the development of a regional mushroom-type interference pattern. As a result, (1) the southwest-trending, steeply overturned Cameron Lake belt dips to the east and faces to the west; (2) in the Sunset subarea, the western and eastern portions of the north-trending synclinal belt, respectively, dip and face inwards; (3) in the Tumpline Lake subarea, the widely intruded, hence complexly folded, volcanic rocks display northwest- and northeast-trending, granitoid-cored, anticlinorial fold axes that collectively wrap around the southern hinge of the Sleepy Dragon complex about a southeast-trending and plunging F2 refold axis (Fig. 1). The resulting lithostratigraphic disposition of the volcanic rocks is complex and locally obscure.

Beaulieu Group volcanic rocks are mainly metamorphosed in amphibolite facies, with the notable exception of a north–northwest-trending, 2–4 km wide, greenschist-facies zone of Alice Formation andesites–dacites–rhyolites within the Sunset Lake syncline, where vthe axis follows the Beaulieu River – Sunset Lake basin system (Fig. 2). Dense swarms or multiple complexes of diabasic–gabbroic dykes and sills at amphibolite-grade metamorphism are widespread within Beaulieu volcanic rocks and subjacent Sleepy Dragon complex (Lambert 1988) (Fig. 1). Near Patterson Lake in the Cameron River subarea (Fig. 2), three distinct swarms are dated at 2734 Ma, 2687 Ma, and in the interval 2683–2660 Ma (Bleeker et al. 1999*b*). Of these, the oldest swarm probably dates the regional rifting of the Central Slave basement complex, an extensional episode that initiated voluminous outpouring of Beaulieu tholeiitic basalts.

Belt setting

In the Cameron River subarea (Fig. 2), the northwesterly overturned volcanic belt forms a steeply dipping homoclinal sequence, which is located at the contact between Sleepy Dragon complex with younger plutonic intrusions to the east and conformably overlying Burwash metaturbidites to the west. Within the map area, the volcanic belt is estimated to be up to 3000 m in stratigraphic thickness (Baragar 1966; Lambert 1988); it tapers abruptly southward to pinch out at Upper Ross Lake, where locally unconformably overlain by Raquette Lake Formation.

In the Sunset Lake subarea (Fig. 2), the northerly trending volcanic belt, ca. 2000–3000 m in stratigraphic thickness, is synclinally folded, as mentioned earlier in the text (see Lambert 1988, fig. 3). The western boundary of this belt, which is mainly in contact with Sleepy Dragon basement, is represented by a gently undulating zone of high ductile strain complicated by mafic dyke swarms and ultramafic units; the eastern margin is similarly marked by sheared contacts and extensive mafic dyke swarms (Fig. 1). Burwash metaturbidites conformably overlie the metavolcanic rocks to the south. Undifferentiated volcaniclastic metasediments, layered schists, and gneisses of the Payne Formation extend to the southeast in lateral facies equivalence (Lambert 1988).

In the Tumpline Lake subarea (Fig. 2), the complexly folded volcanic belt, possibly ca. 2400 m thick (Lambert 1988), extends eastward from Victory Lake to Tumpline Lake, thence northward to Rex Lake. The volcanic rocks lie mainly in structural contact with basement gneisses to the north and are mainly overlain conformably by Burwash

Fig. 2. Geologic map of the Cameron River – Beaulieu River area, with locations by subarea of 51 re-analyzed volcanic samples and three main mineral deposits and properties. Mafic dyke swarms, shown in Fig. 1, are omitted for clarity. The Payne Lake Formation (clear) is considered to be laterally transitional with the main Beaulieu River belt. Adapted from Lambert (1977, fig. 1). BIF, banded iron formation; Fm., Formation.

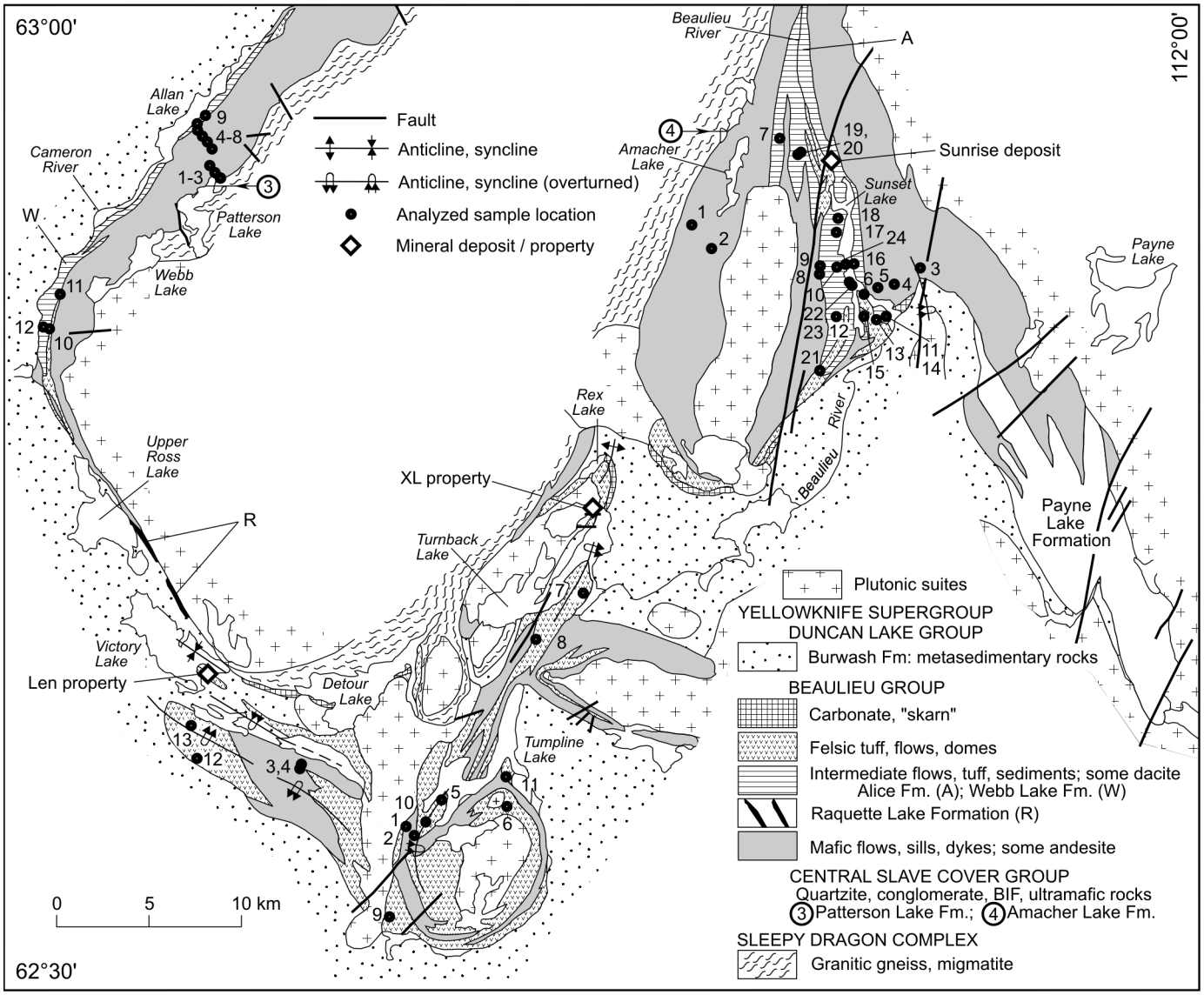

metaturbidites to the south. Numerous strata-intruding, elliptical–subcircular granitic masses have produced unusually complex structures, resulting in variable lithostratigraphic interpretations.

Lithostratigraphy

Central Slave Cover Group

Thin, discontinuous Central Slave Cover Group formations, composed of highly strained conglomerate with occasional spinifex-textured ultramafic volcanic clasts, fuchsitic quartzite, turbiditic grits, and BIF are exposed at Patterson and Amacher lakes in the Cameron River and Sunset Lake subareas, respectively (Fig. 1). In the Yellowknife area, 110 km to the west, lithologically similar Bell Lake and Dwyer Lake formations underlie Yellowknife belt volcanic rocks (Fig. 1).

Beaulieu Group

In brief, the Cameron River and Beaulieu River greenstone belts are each characterized by a lower tholeiitic package dominated by pillowed basalt, mafic dykes and sills, and an upper calc-alkaline package with mainly flows and breccias of andesite, dacite, and rhyolite. Mafic–felsic tuffs and sedimentary rocks form minor components (Ketchum et al. 2004).

Following Lambert (1988, figs. 1, 2), within both Cameron Lake and Sunset Lake subareas (Fig. 3), thick dominantly tholeiitic basalt formations (named Cameron River basalt and Sunset Lake basalt, respectively) are overlain by broadly lensoid calc-alkaline, Rhyolite and Webb Lake andesite in the Cameron lake subarea and Alice andesite–dacite and Rhyolite in the Sunset Lake subarea. The southeastern extension of the Sunset Lake belt (Fig. 2) is underlain by Payne Lake epiclastic–metavolcanic rocks. In the intervening Tumpline

Lake subarea, the complexly folded volcanic assemblage is considered by Lambert (1988) to comprise (1) Tumpline basalt flows, including andesite and dacite members, with (2) overlying Sharrie and Turnback rhyolite domes, each measuring up to 850 m thick and 10 km long, and (3) bedded carbonate–skarn–tuff-pyritic gossan distributed along the south shore and nearby islands of Detour Lake, as well as in the Rex Lake vicinity to the northeast (Fig. 2). The gossans have been variably interpreted as (1) pre-volcanic Detour Lake Group (Kusky 1990); (2) lateral continuations of the Cameron River volcanic belt (Mueller and Corcoran 1997); (3) intravolcanic Detour Lake Formation, correlated with Raquette Lake Formation to form the Detour Lake Group (Bleeker 2001); and (4) final waning volcanic exhalations (Lambert 1988).

The abrupt Cameron River belt tapering in the Upper Ross – Victory Lake interval (Fig. 2) is attributed by Bleeker (2002) to two relationships: (1) Cameron River basalts were intruded along their base by a generally coeval, i.e., ca. 2700 Ma pluton (Ross Lake granodiorite); and (2) Cameron River basalts were consequently tilted and eroded along a developing intravolcanic unconformity, such that the younger overlying calc-alkaline volcanic assemblage, itself dated by 2663 Ma old porphyritic units (Henderson et al. 1987), progressively cuts out the older Cameron River basalt. According to Bleeker (2001), to the southeast this intravolcanic unconformity is marked by the Raquette Lake Formation (2683–2661 Ma), which is a heterogeneous assemblage up to 250 m thick of conglomerate, quartzitic arenite, felsic tuff, and calc-silicates that represent part of a proposed craton-scale overlap sequence. To the northeast, this intravolcanic unconformity, at the base of the younger volcanic sequence, cuts up stratigraphy again to allow the reappearance within the Sunset Lake subarea of the older underlying tholeiitic package in the form of the Beaulieu River basalts.

Therefore, two discreet volcanic sequences are present in the CR–BR region, at least 13 million years apart, and separated by granodiorite intrusions and partial doming with subsequent erosion. Of the two, the older tholeiitic basalt sequence is apparently largely present only in the Cameron River and Sunset Lake subareas, whereas the younger intermediate–felsic–rich volcanic sequence is present in all three subareas (Bleeker 2002).

Mineralization

Numerous mineral showings, mainly barren sulphide occurrences, are widely distributed in CR–BR volcanic rocks (see Lambert 1988, figs. 2, 3). Significant base-metal sulphide occurrences are located in upper felsic volcanic-rich horizons in both Tumpline Lake and Sunset Lake subareas (Franklin 1996; Atkinson 1990). The most common sulphide minerals are sphalerite, galena, pyrite and arsenopyrite. Sulphide lenses typically grade laterally and vertically into chert, carbonate, and carbonaceous argillite (Atkinson 1990). No significant gold mineralization has been reported.

The XL property at the northeast end of Turnback Lake (Fig. 2) contains sulphide mineralization at a north-trending contact between Burwash metasediments and rhyolite–carbonate skarn. The calculated resource is 180 000 t at a grade of 6% Zn, 2% Cu, 1.5% Pb, and 103 g Ag/t to a depth of 90 m (NORMIN File Showing Id. 085INE0023). A nearby, 2 m × 10 m secondary zone is reported to contain 8.4% Pb, 13.7% Zn and 644g Ag/t (NORMIN File Showing Id. 085INE0023).

The Len property, at the southeast end of Victory Lake, contains a narrow, northwest-striking andesite–rhyolite belt (2670 Ma) in contact with overlying Burwash metasediments. A gossanous zone, 100 m × 30 m, contains disseminated Zn–Cu-bearing sulphide minerals. No resource estimate is available.

In the Sunset Lake subarea (Fig. 2), the extensively explored and drilled Sunrise volcanogenic massive sulphide (VMS) deposit lies within north-trending rhyolite–andesite units at the extreme north end of Sunset Lake. The ore deposit includes both an upper, massive lens of high-grade sphalerite–galena–pyrite and a much larger underlying, lower grade, footwall zone of disseminated sulphides. The upper high-grade lens contains proven ore resources of 1 865 699 t grading 403 g Ag/t, 1 g Au/t, 0.1% Cu, 4.2% Pb, and 8.9% Zn. The underlying, lower grade sulphide zone ranges from 2% to 10% combined Pb–Zn, with up to 100 g Ag/t (Franklin 1996). The nearby, much smaller and lower grade Bear deposit, located 1 km to the south across the intervening Campsite fault, reports resources of 809 700 t (Franklin 1996).

Geochemistry

During field mapping in the CR–BR area (Lambert 1988), 117 composite chip samples were collected and subsequently analyzed for major and some minor elements in the laboratories of the Geological Survey of Canada, Ottawa, Ontario. Fifty-one of the samples were re-analyzed for minor and trace elements in the Department of Geology, University of Toronto (Table 1).Their approximate field and stratigraphic locations are shown by subarea (Figs. 2, 3). The analytical techniques employed and the precision of the results are described in detail elsewhere (Barnes and Gorton 1984). Chondrite values used throughout to normalize rare-earth element (REE) abundances are those by Taylor and Gorton (1977).

Despite chemical alteration problems in metamorphosed rocks, a simple SiO_2-based (volatile-free basis) rock classification is used as follows: basalt = < 53%, basaltic andesite = 53%–57%, andesite = 57%–63%, dacite = 63%–70%, rhyolite = > 70% SiO_2. The pertinent resulting CR–BR chemical results are tabulated by (1) trace and minor element contents by individual sample (Appendix A); and (2) mean class composition by subarea (Table 1). The results are further illustrated and interpreted by means of derived plots and diagrams (Figs. 3–5).

In general, late Neoarchean volcanic rocks in the CR–BR and Yellowknife areas (further considered later in the text) correspond closely in chemical composition to coeval volcanic classes elsewhere (Baragar 1966; Condie and Baragar 1974; Condie 1976; Goodwin 1979; Thurston et al. 1985; Polat and Kerrich 2001).

Cameron River – Beaulieu River volcanic rocks have the following minor and trace element characteristics: (1) in basalt and basaltic andesite: low, flat REE patterns; weakly negative to moderately positive Eu anomalies; low to moderate Y, Sr, and high field-strength elements (HFSE) (Ta + Zr +

Table 1. Mean class composition by subarea of volcanic rocks in the Cameron River – Beaulieu River area.

	Beaulieu Group														
Subarea:	Cameron River					Tumpline Lake					Sunset Lake				
Class:	Basalt	Basaltic andesite	Andesite	Dacite	Rhyolite	Basalt	Basaltic andesite	Andesite	Dacite	Rhyolite	Basalt	Basaltic andesite	Andesite	Dacite	Rhyolite
Column:	1	2	3	4	5	6	7	8	9	10	11	12	13	14	15
n:	8	2	2	1	1	1	1	1		9	6	3	8	3	4
SiO_2 (wt.%)	50.92	55.64	59.38	67.78	74.47	51.24	55.20	61.75	65.00	77.34	51.43	54.02	59.71	63.55	81.26
TiO_2	1.44	1.35	1.03	0.73	0.03	1.65	1.29	1.40	1.50	0.23	1.10	1.02	1.10	0.89	0.10
Al_2O_3	15.43	14.66	14.83	14.67	16.48	15.13	15.89	12.27	12.30	11.63	16.33	16.86	16.54	15.68	10.89
FeO*	12.19	9.93	7.66	4.80	1.29	11.89	10.56	11.89	9.09	1.76	10.45	10.36	7.25	5.92	0.96
MnO	0.26	0.27	0.16	0.08	0.04	0.22	0.19	0.25	0.23	0.05	0.28	0.39	0.16	0.15	0.02
MgO	5.92	3.71	4.56	2.83	2.66	4.88	4.14	1.69	1.60	0.88	6.40	5.65	4.50	2.85	0.66
CaO	11.19	11.68	8.09	2.78	0.68	10.70	9.59	7.30	4.74	1.73	10.14	8.41	5.34	5.85	1.17
Na_2O	2.06	2.47	3.15	3.28	0.33	3.14	2.38	2.41	4.16	3.21	2.91	2.67	3.84	3.77	2.47
K_20	0.39	0.14	0.32	0.19	0.03	0.33	0.26	0.56	0.57	0.10	0.16	0.12	0.27	0.25	0.03
P_2O_5	0.18	0.14	0.32	0.19	0.03	0.33	0.26	0.56	0.57	0.10	0.16	0.12	0.27	0.25	0.03
FeO*/MgO	2.13	2.68	1.71	1.70	0.48	2.44	2.55	7.04	5.68	3.05	1.80	1.96	1.86	2.23	1.81
FeO*/(FeO* + MgO)	0.67	0.72	0.63	0.63	0.33	0.71	0.72	0.88	0.85	0.68	0.61	0.64	0.63	0.68	0.59
La (ppm)	8.2	7.7	22.3	46.1	12.7	15.3	9.3	25.7	31.2	49.5	9.4	7.3	23.4	18.9	48.8
Ce	22.7	17.4	51.2	92.0	26.6	33.2	24.7	68.0	67.3	96.5	21.5	13.9	47.6	40.3	108.9
Nd	11.3	11.0	22.1	20.7	9.4	18.4	8.4	25.8	26.1	34.1	9.0	7.0	18.2	14.6	37.3
Sm	4.0	3.8	5.7	6.3	3.8	4.4	3.0	7.0	7.6	8.5	3.3	2.6	4.5	4.1	8.7
Eu	2.0	1.0	2.7	3.8	0.4	1.3	1.0	3.6	1.5	1.4	2.0	0.8	2.0	1.9	1.5
Eu_N	27.9	13.9	38.1	53.3	5.2	17.8	13.8	50.6	20.2	19.2	28.0	11.2	28.3	25.8	20.3
Eu^*_N	18.8	18.9	25.3	27.0	18.4	19.5	14.8	32.5	34.5	35.1	16.0	14.1	20.6	18.8	37.4
Tb	0.8	0.9	0.9	0.9	0.8	0.7	0.7	1.3	1.3	1.4	0.7	0.7	0.8	0.6	1.4
Ho	1.5	1.1	1.5	0	0	1.37	0.9	1.6	1.8	1.3	1.1	1.6	1.0	0.7	1.2
Yb	2.7	3.2	3.9	2.5	3.4	2.81	2.2	4.5	4.8	6.9	2.8	2.6	2.6	2.0	4.53
Lu	0.4	0.5	0.6	0.3	0.5	0.4	0.4	0.1	0.8	0.7	0.4	0.4	0.4	0.3	0.7
$\sum$ REE	53.7	46.6	110.9	172.7	57.6	77.9	50.5	137.7	142.4	200.3	50.3	37.0	100.6	83.4	213.1
$(Yb)_N$	12.0	15.3	18.8	11.9	16.5	13.5	10.6	21.4	23.2	32.9	13.7	12.3	12.3	9.8	21.8
Th	0.9	0.7	4.7	29.8	22.6	2.1	1.9	12.7	12.4	17.9	2.8	2.3	4.6	5.5	22.6
Hf	3.0	2.6	5.1	5.7	3.1	2.7	2.3	6.9	6.7	6.6	2.5	2.0	3.9	4.0	5.9
Ta	0.4	0.2	0.7	1.2	1.0	0.4	0.4	1.1	0.9	1.1	0.3	0.2	0.5	0.6	1.0
Ba	81	0	254	416	157	86	102	60	106	968	182	34	267	181	528
Sc	42.0	38.4	31.0	12.7	1.9	34.4	35.5	23.6	25.2	5.5	39.0	38	20.0	14.9	3.4
Co	56	38	39	15	1	43	45	17	17	2	47	45	23	16	1
Cr	177	115	167	53	2	137	149	6	3	3	218	236	92	55	2
Ni	97	62	76	20	1	72	87	2	1	3	124	123	47	25	4

Table 1 (*concluded*).

Subarea:	Beaulieu Group													
	Cameron River					Tumpline Lake					Sunset Lake			
Class:	Basalt	Basaltic andesite	Andesite	Dacite	Rhyolite	Basalt	Basaltic andesite	Andesite	Dacite	Rhyolite	Basalt	Basaltic andesite	Andesite	Dacite	Rhyolite
Column:	1	2	3	4	5	6	7	8	9	10	11	12	13	14	15
n:	8	2	2	1	1	1	1	1		9	6	3	8	3	4
V	283	295	166	90	3	304	246	59	57	8	246	258	184	119	3
Zr	91	105	174	200	75	125	111	251	276	233	99	83	181	174	180
Y	26	31	33	30	41	30	24	48	50	57	28	27	28	23	49
Sr	185	125	160	189	57	198	164	195	152	96	140	132	183	236	63
Rb	17	1	19	127	209	17	15	6	21	99	23	5	22	17	73
$(La/Yb)_N$	1.8	1.5	3.9	12.3	2.5	3.6	2.8	3.8	4.3	6.1	2.0	1.9	5.7	6.7	7.3
Eu/Eu*	1.5	0.7	1.5	2.0	0.3	0.9	0.9	1.5	0.6	0.6	1.7	0.8	1.4	1.4	0.5
Zr/Y	3.5	3.3	5.4	6.7	1.8	4.2	4.6	5.2	5.5	4.1	3.4	3.1	6.5	8.0	3.8
Rb/Sr	0.07	0.02	0.12	0.67	3.67	0.09	0.09	0.03	0.14	1.92	0.18	0.04	0.15	0.10	1.32

Hf); high Sc. (2) in andesite and dacite: gently sloping, moderately enriched REE patterns; moderately positive Eu anomalies; moderate Y, Sr, and HFSE; high Sc. (3) In rhyolite: moderately sloping, substantially enriched REE patterns; pronounced negative Eu anomalies; low Sr and Sc; high HFSE.

Mean class compositions of volcanic rocks by subarea (Table 1)

Within the CR–BR area, Sunset Lake basalt + basaltic andesite + andesite in the east, compared with Cameron River volcanic class equivalents in the west, contain higher AI_2O_3, Na_2O, and K_2O and lower CaO, Sc, and REEs, which in part reflects the presence of high-Al_2O_3 basalts in the Sunset Lake subarea (Lambert 1988). The data suggest, in brief, that the mafic–intermediate volcanic sequence in the easterly disposed Sunset Lake subarea is more evolved in the direction of arc-type volcanic assemblages.

AFM relations (Fig. 3)

AFM ((Na_2O + K_2O)–FeO–MgO) diagrams of the three subareas indicate that (1) the Cameron River belt contains mainly tholeiitic basalts with modest andesite and rare alkali-poor felsic associates; (2) the Tumpline Lake subarea sequence, as sampled, is pronouncedly bimodal (tholeiitic basalt – calc-alkaline, dacite–rhyolite); and (3) Sunset Lake volcanic rocks of Beaulieu River belt represents a more fully developed tholeiitic basalt – calc-alkaline, intermediate–felsic volcanic sequence that is more comparable to modern arc-type assemblages.

Felsic volcanic rocks in both Tumpline Lake and Sunset Lake subareas are chemically similar, thereby supporting their proposed stratigraphic correlation. Also, both subareas include significant proportions of high-SiO_2 (77%–81%) rhyolites that compare closely in critical chemical components, viz. SiO_2, $(La/Yb)_N$, Zr/Y, Rb/Sr, and Eu/Eu*, to high-silica rhyolites in the Abitibi belt of the Superior Province, southern Canadian Shield (Barrie 1995). Abitibi rhyolites provided zircon saturation temperatures of volcanic extrusion of 840–940 °C (Barrie 1995). Correspondingly, high extrusion temperatures may have existed in the Sunset–Tumpline lakes subareas of the CR–BR area.

Th–Zr–REE relations (Fig. 4)

Ujike and Goodwin (1987) used the ratios 100 × Th/Zr versus $(La/Yb)_N$ as a useful petrogenetic tracer in the study of felsic volcanic rocks (>62% SiO_2) in the Noranda area of the Superior Province, southern Canadian Shield (further considered later in the text). They demonstrated that Noranda felsic metavolcanic rocks have mutually low 100 × Th/Zr (<2) and $(La/Yb)_N$ (<5) ratios, which place them very close to the composition of primitive Earth mantle (PM) but significantly removed from average Archean total crust (AATC). This supports the argument that these particular felsic volcanic rocks are products of shallow-level fractional crystallization of mafic parental magmas formed by partial melting of a primitive mantle source, with negligible contribution to magma genesis from plausible crustal materials.

However, CR–BR and Yellowknife mafic–intermediate–felsic metavolcanic rocks (Fig. 4) show markedly different relationships: (1) mean CR–BR and Yellowknife basalt both plot midway between PM and AATC, suggesting mainly

Fig. 3. AFM diagrams by subarea showing the distribution of tholeiitic (TH) and calc-alkaline (CA) series, as separated in the figure by upward convex line. Upper-left sequential listings by subarea show the numbered distribution of re-analyzed samples by stratigraphic formation/member. Lower-right listings by subarea show the reanalyzed sample numbers, and corresponding original field number (Lambert 1988), together with volcanic class and series designations: bs, basalt; bs-an, basaltic andesite; an, andesite; dc, dacite; ry, rhyolite. Fm., Formation; Mbr., Member. Volcanic class symbols within AFM diagrams by subarea: basalt + basaltic andesite, open square; andesite, filled circle; dacite, open circle; rhyolite, filled triangle.

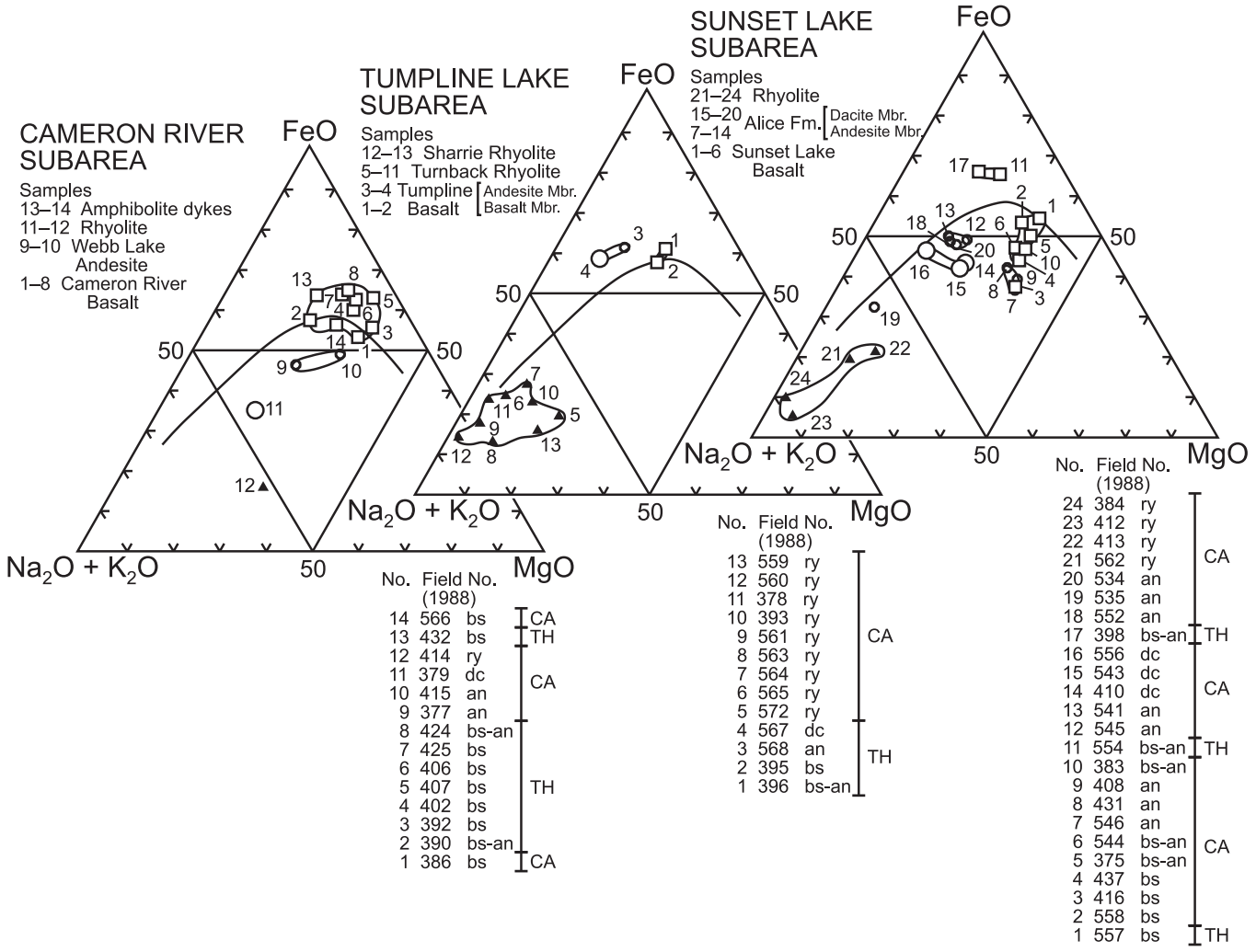

mantle derivation with possibly minor crustal contamination; (2) mean CR–BR and Yellowknife andesites plot, respectively, at, and close to, AATC, thereby suggesting significant crustal contributions; and (3) mean CR–BR dacite and rhyolite, as well as mean Yellowknife dacite, all plot close or marginal to the plot of felsic metavolcanic samples from three widely dispersed regions—Barberton Mountain Land, Transvaal, Africa (Glikson 1976); Pilbara block and Marda complex, western Australia (Jahn et al. 1981; Taylor and Hallberg 1977); and Bababudan belt, India (Drury 1983). All three are confidently attributed to partial melting of Archean crust. Accordingly, similar crustal melting contributions may apply to CR–BR and Yellowknife felsic volcanic petrogenesis.

$(La/Yb)_N$ versus $(Yb)_N$ relations (Fig. 5)

This figure illustrates the abundance trend of light (La) and heavy (Yb) REEs during progressive stages of magma petrogenesis. In general, a steep upward $(La/Yb)_N$ development is called a "high La/Yb" trend, whereas a flattish rightward $(Yb)_N$ development is called a "high Yb" trend. The main cause of contrasting "high La/Yb" and "high Yb" trends is attributed to the presence or absence of garnet ± amphibole in the residue of differentiating magmas.

Rare-earth element results are plotted by individual CR–BR subarea (Figs. 5A–5C) and, together with corresponding Yellowknife REE results (Goodwin 1988; Cousens 2000; Cousens et al. 2002), by collective southern Slave Province composite (Fig. 5D). Considered by subarea, Cameron River and Sunset Lake basalts plot in similar field *III* positions (Figs. 5A, 5C), which supports their proposed stratigraphic correlation; in contrast, Tumpline Lake basaltic rocks (Fig. 5B) plot in field *II*, suggesting a more evolved petrogenesis.

The overall CR–BR intermediate–felsic volcanic pattern displays a flattish rightward "high Yb" trend (Fig. 5D: fields *II, V, VI*), whereas the Yellowknife pattern displays a steeply upwards "high La/Yb" trend (Fig. 5D: fields *I, II*). The con-

Fig. 4. 100 × Th/Zr – $(La/Yb)_N$ plots of Cameron River – Beaulieu River (CR–BR) belts and Yellowknife belt average composition by volcanic class; felsic volcanic samples from Noranda area (Abitibi belt, Superior Province); and felsic volcanic samples from Barberton Mountain Land, South Africa (Glikson 1976), Pilbara, block Australia (Jahn et al. 1981), and Bababudan belt, India (Drury 1983). All plots relative to plots of primitive Earth mantle (PM) and average Archean total crust (AATC). Volcanic class designations as in Fig. 3.

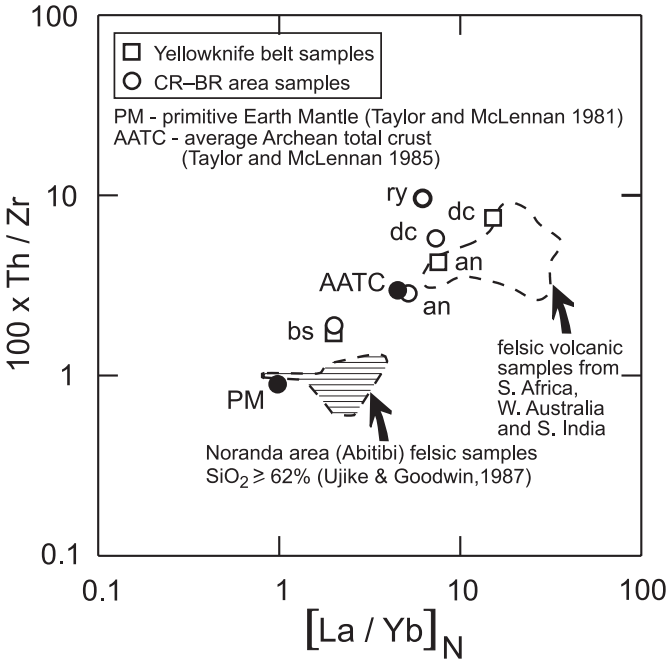

trasting "high Yb" and "high La/Yb" volcanic trends, which are also referred to, respectively, as "classic calc-alkaline" and "adakitic," have distinctive petrogenetic, tectonic, and metallogenic implications, as considered as follows:

(1) High-pressure melting experiments by Rapp et al. (1991) indicated that favourable conditions for extraction of intermediate–felsic magma with "high La/Yb" trend is by vapour-absent, partial melting of an eclogite or amphibolite source at pressures between 16 and 32 kbar (1 kbar = 100 MPa), and optimally 22 kbar, i.e., ca. 66 km depth, owing to selective retention of Yb by garnet + amphibole in the crystalline residue. Further partial melting experiments on amphibolites by Rapp and Watson (1995) suggested that both Archean TTG and modern adakites can be generated by 10%–40% melting of thick, partially hydrated metabasaltic crust at temperatures between 1000 and 1100 °C and pressures > 12 kbar, i.e., ca. > 30 km depth. In this regard, as defined by Martin et al. (2005), adakites form a distinct suite of intermediate to felsic rocks (e.g., andesite–dacite–rhyolite), with basaltic members notably lacking; a salient characteristic feature is that REE patterns are strongly fractionated with $(La/Yb)_N > 10$, with typically low heavy REE contents.

(2) Martin (1987, 1999) demonstrated that the Archean TTG series, which forms some 90% of the common Archean crust, also is characterized by "high La/Yb" trends. Tonalite–trondhjemite–granodiorite development is practically, though not entirely, restricted to Archean time. This temporal restriction is commonly attributed to a long-term, progressively cooling mantle (Martin 1986; Martin and Moyen 2002). Martin (1987) viewed Archean "high La/Yb" volcanic rocks, i.e., adakites, as extrusive equivalents of Archean TTG suites.

(3) Martin et al. (2005), using a greatly expanded TTG geochemical database, confirmed that the chemical composition of TTG magmas has evolved across Archean time (4.0–2.5 Ga), with measurable increases in each of two groups occurring at about 3.0 Ga: (1) Mg#, Ni, and Cr, and (2) CaO, Na_2O, and Sr. The respective group increases are attributed to (1) progressively increased interaction between metabasalt-generated felsic melts and mantle peridotite, and (2) the decreasing amount of plagioclase, residual from basalt melting, in reponse to increased pressures at the site of melting. Both compositional changes are attributed to the progressively deeper melting of subducting crust in response to the decreasing geothermal gradient across Archean time.

Furthermore, examination of the accompanying adakite geochemical database (Martin et al. 2005) identified two distinct compositional groups: (1) high-silica adakites (>60% SiO_2), considered to represent subducted basaltic slab-melts that have reacted with peridotite during ascent through the mantle wedge; and (2) low-silica adakites, attributed to melting of peridotitic mantle wedge with its composition partly altered by felsic slab-melts. It is noted here that all the late Neoarchean Canadian Shield adakites herein considered belong to the high-SiO_2 category. Martin et al. (2005) concluded that the close compositional similarities between late Archean (3.0–2.5 Ga) TTG and high-SiO_2 adakites strongly suggest a direct petrogenetic analogy.

(4) Modern examples of "high La/Yb"-trend volcanism are represented by rare adakitic volcanic rocks (Martin 1999; Defant and Drummond 1990; Defant and Kepezhinskas 2001; Samaniego et al. 2002). Most are directly related to subduction processes, where the young (<20 Ma) and still hot subducted plate is located 70–90 km beneath the volcanic arc, itself composed of predominant classic calc-alkaline volcanic suites.

(5) Classic calc-alkaline – adakitic magma transitions may be complexly variable over time and space, depending on sensitive compositional and geodynamic controls (Rapp et al. 1999; Yogodzinski et al. 2001; Samaniego et al. 2002; Garrison and Davidson 2003). As a result, a volcanic assemblage may include abrupt classic calc-alkaline – adakitic transitions both along and across strike. Interpreting magma genesis effectively requires sophisticated, three-dimensional knowledge of syn-volcano-tectono-stratigraphic relations. In general, the older the volcanic terrain, the greater the interpretative challenge.

Yellowknife greenstone belt

Belt setting and lithostratigraphy

The Yellowknife greenstone belt, located 110 km to the west of CR–BR belts, is composed of a north-trending, 10–12 km thick, tholeiitic basalt-rich succession (Baragar 1966; Helmstaedt and Padgham 1986; Goodwin 1988; Padgham 1990; Cousens 2000; Cousens et al. 2002; Martel et al. 2002).

Fig. 5. $(La/Yb)_N$ – $(Yb)_N$ plots of Cameron River – Beaulieu River (CR–BR) volcanic samples by subarea (5A–5C), and of combined Yellowknife + CR–BR belts composite (5D). The division of the figure into fields *I–Vl* mark out general compositional boundaries of major volcanic classes, e.g., field *III*, most basalts. Data used in Capdevila et al. (1982); Lesher et al. (1986); Ujike and Goodwin (1987, 2002). The pre-1986 nomenclature of the Yellowknife belt after Baragar (1966); post- 1986 nomenclature after Helmstaedt and Padgham (1986). Volcanic class and other symbols as in Fig. 3.

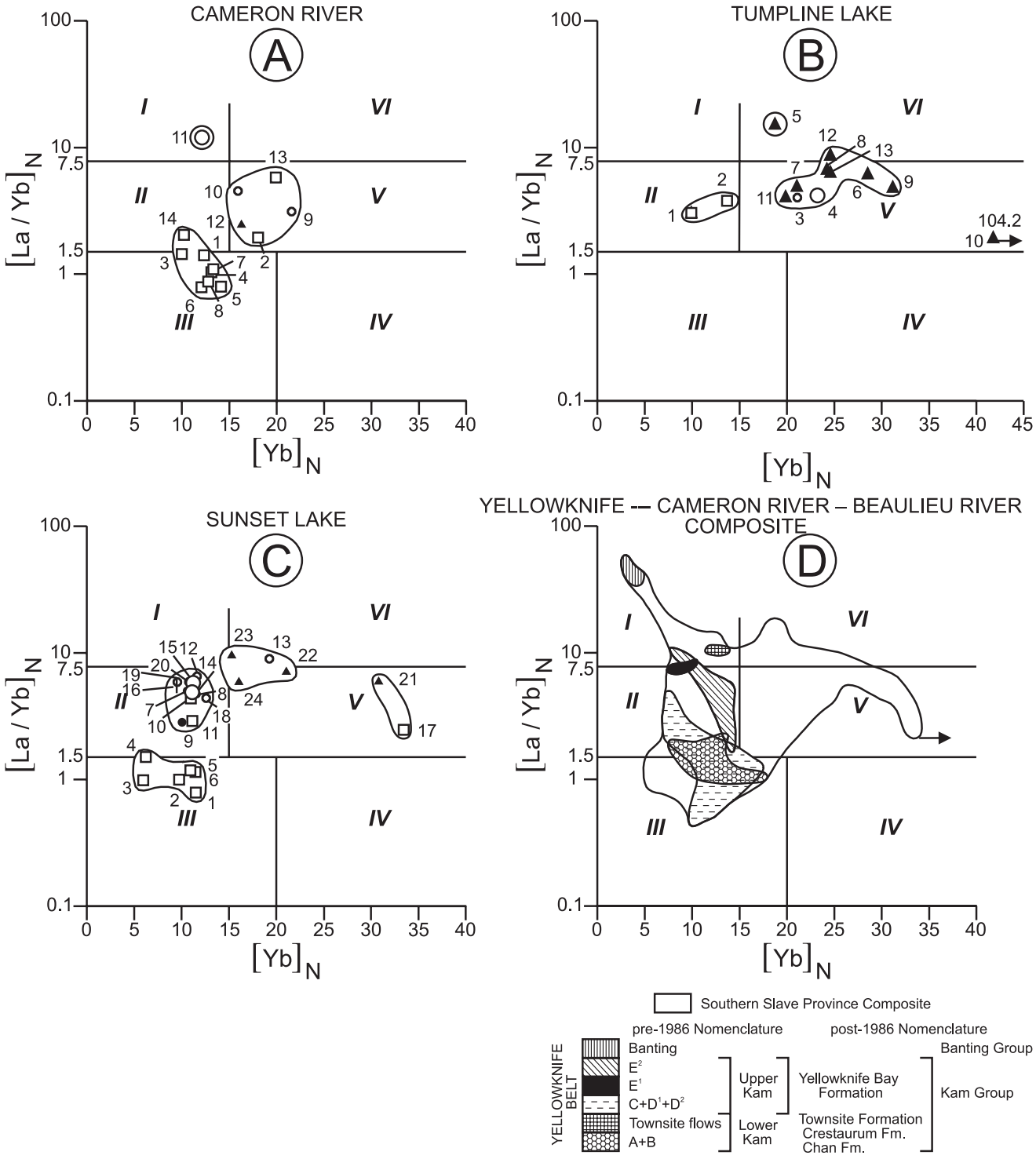

The formerly northeast-trending, southeast-facing belt is cut by numerous north-trending, subvertical, left-lateral faults to form the present northerly trending, near-vertical greenstone belt (Fig. 1). The volcanic rocks are mainly metamorphosed to the greenschist facies. To the west, the belt is intruded by the western plutonic granitoid complexes (2641–2608 Ma);

to the east, it is conformably overlain by Burwash metaturbidites of the Duncan Lake Group.

The Yellowknife belt is also divided into lower tholeiitic and upper calc-alkaline packages. The older, ca. 10 km thick, tholeiitic basalt-rich Kam Group (2712–2701 Ma) is overlain by the younger, thinner (ca. 700 m thick), felsic pyroclastic-rich Banting Group (2664–2658 Ma). The Kam–Banting contact has been traditionally interpreted as an unconformity (Helmstaedt and Padgham 1986) with a depositional gap in the order of 40 million years. (Isachsen and Bowring 1997). The Kam and Banting groups, in turn, are unconformably overlain by a thin, steeply dipping, east-younging, metaconglomerate–sandstone panel of the Jackson Lake Formation (<2605 Ma; Isachsen 1992), which is a typical Timiskaming-type, "pull-apart," sedimentary formation (Jirsa 2000).

The older Kam Group is divided into four conformably overlying formations (Fig. 5D, lower right listings) (Helmstaedt and Padgham 1986; Cousens 2000): (1) Chan Formation, the thickest (ca. 6 km), is composed entirely of basaltic lava flows with prominent basal dyke-and-sill complex; (2) Crestaurum Formation is rich in pillow basalt flows, with several thin, cherty, dacitic interbands; (3) Townsite Formation is uniquely dominated by dacitic–rhyolitic flows, tuffs and breccias; and (4) Yellowknife Bay Formation, up to 5 km thick, is mainly composed of pillow basalt flows and sills, with several intercalated cherty tuffaceous units.

The younger Banting Group is dominated by assorted felsic porphyries, breccias, fragmental flows, and bedded tuffs, with minor mafic–intermediate flows. Near the top of the sequence, several possibly subaerial ash-flow units with fiamme and relic glass shards have been recognized (Helmstaedt and Padgham 1986).

Mineralization

The Yellowknife belt ranks as a former world-class gold producer. Major late-stage, shear-zone-hosted, lode-gold deposits are effectively confined to the Yellowknife Bay Formation of the Kam Group (Padgham 1990). Mineralization consists of broad zones of silicification and quartz–carbonate veining, which form gold–quartz alteration systems. The dominant Giant Yellowknife Mine produced 189 t of gold from 13.9 million t of ore grading 17.8 g/t.

Although highly controversial in origin (see further later in the text), a popular genetic model attributes the lode-gold mineralization to vertical migration of metamorphically derived, auriferous fluids through a vertical system of anatomizing shear zones, with gold veins deposited in favourable dilatant zones (Boyle 1953; Kerrich 1990; Van Hees et al. 1999; Siddorn and Cruden 2000).

Geochemistry and petrogenesis

Kam Group

Mafic volcanic rocks in all formations follow common tholeiitic fractionation trends (Cousens 2000). Associated Nd values indicate a depleted mantle source, followed by some degree of interaction with older crust (Isachsen and Bowring 1997). Associated intermediate–felsic units, which are strongly enriched in light REEs, also indicate contamination by older crustal rocks, such as basement granitoids (Cousens 2000).

Banting Group

Basaltic rocks of this group, also with common tholeiitic trends, are interpreted to represent melts of depleted upper mantles (Cousens et al. 2002). However, Banting intermediate–felsic volcanic rocks are adakitic in composition (Fig. 5D). They are attributed to 5%–10% partial melting of an amphibolite–granulite-grade, basaltic source, leaving small amounts of garnet in the residue (Jenner et al. 1981).

Isachsen and Bowring (1997) further stressed that the presence of inherited zircons in the lower Kam Group provides additional evidence that the Yellowknife greenstone belt is largely autochthonous with repect to older basement.

In both the Yellowknife and Cameron River volcanic belts, Baragar (1966) attributed the earlier tholeiitic mafic trends to crystal fractionation in high-level, mantle-derived magma chambers, and the later calc-alkaline intermediate–felsic trends to progressive contamination of tholeiitic magma by sialic crust

Southern Slave Province greenstone composite

Southern Slave Province volcanic belts reveal a dual volcano-metallotectonic relationship, as follows: (1) CR–BR volcanic belts in the east are characterized by comparatively thin, moderately deformed, classic calc-alkaline volcanic flow-rich sequences, with associated syngenetic base-metal VMS ore deposits; whereas (2) the Yellowknife belt, 110 km to the west, is characterized by a comparatively thick, structurally complex, lower tholeiitic flow sequence unconformably overlain by a pyroclastic-rich adakitic sequence with associated late-stage, mesothermal, lode-gold deposits. Salient characteristics are summarized in Fig. 6.

This volcano-metallotectonic duality is not unique to the southern Slave Province, but it is matched in at least two similar coeval greenstone regions of the Superior Province: the southern Canadian Shield (Fig. 7, inset map), as briefly summarized later in the text, the Karelian greenstone belts of the Baltic Shield (Samsonov at al. 2005), and elsewhere (Boily and Dion 2002; Daigneault et al. 2004; Manikyamba et al. 2005). In brief, this volcano-metallotectonic greenstone duality may prove to be a common late Neoarchean characteristic.

Lake of the Woods – Wabigoon region, western Superior Province

Belt setting and lithostratigraphy

The east-trending, 200 km long Lake of the Woods – Wabigoon Lake region (Fig. 7, inset map) forms the northwest third of the east-trending Wabigoon subprovince (Goodwin 1965, 1977; Davis et al. 1988; Davis and Smith 1991; Blackburn et al. 1991; Ayer and Davis 1997; Ayer and Dostal 2000; Ujike and Goodwin 2002). The region is underlain by continuous structurally deformed Keewatin metavolcanic rocks (2743–2711 Ma) and overlying metaturbidites (2714–2696 Ma), with granitoid plutonism and deformations (2711–2685 Ma). Stratigraphic thicknesses range from > 20 km in the west to > 10 km in the east. The common metamorphic grade is greenschist facies.

Fig. 6. Salient lithologic–metallogenic characteristics in the southern Slave Province greenstone belts, together with petrogenetic characteristics by region.

	Adakitic volcanic rocks (west) ← Yellowknife Belt (120 km)	Classic calc-alkalic volcanic rocks → (east) Cameron River – Beaulieu River Belt
Extrusive rocks - Salient Features:	1. Thick, tholeiitic basalt-dominated flow sequences with unconformably overlying pyroclastic-rich adakites 2. "High La/Yb" pattern; high Sr, Zr/Y, Sc; low HFS elements; positive Eu anomalies 3. Deformed volcanic rocks cut by major fault-shear zones	1. Thin, interlayered basalt-andesite-dacite-rhyolite lava flow sequences; major rhyolites, including high-SiO_2 varieties 2. "High Yb" pattern; low Sr, Zr/Y, Sc; high HFS elements; pronounced negative Eu anomalies 3. Moderately deformed volcanic rocks
Degree of Magma Fractionation:	Limited	Substantial; in shallow - level magma chambers
Rate of Magma Ascent:	Fast	Slow
Main Mineralization	Mesothermal, late-stage, lode gold deposits; mainly in unconformity-related volcanic group; associated with late fault-shear zones	Syngenetic, base-metal VMS seafloor or sub-seafloor deposits; at or near preferred felsic volcanic contacts

In the western area (Lake of the Woods), the 10 km thick, tholeiitic, basalt-rich Lower Keewatin assemblage (2738–2732 Ma) is disconformably overlain by the equally thick, tholeiitic–calc-alkaline Upper Keewatin assemblage (2723–2719 Ma). The uncomformably overlying electrum metaturbidites (2714–2696 Ma) include local volcanic shoshonites (alkaline), the latter coeval with nearby ultrapotassic plutons (Ayer and Dostal 2000).

In the adjoining central area (Long Bay – Kakagi Lake), remnant patches of basalt-rich lower Keewatin volcanic equivalents are overlain by substantial thicknesses of calc-alkaline, mafic–felsic upper Keewatin volcanic equivalents. Ultramafic sills (2725 Ma) are unusually common.

In the eastern area (Wabigoon–Manitou lakes), Lower Keewatin tholeiitic basalt-rich volcanic equivalents are locally underlain by still older Archean tholeiitic volcanic units (to 2743 Ma), and extensively overlain by calc-alkaline-rich Upper Keewatin volcanic equivalents.

Mineralization

Mineralization in the Lake of the Woods – Wabigoon region is varied in type, but with only limited past production (late 1800s – early 1900s). Gold production was mainly restricted to the Lake of the Woods area in the west, with production per mine ranging from 1000 to 77 000 t milled at average grade of 10.7 g/t Au and 1.33 g/t Ag. Gold deposits are related to late shear zones and contact strain aureoles marginal to granitoid intrusions. The age of gold mineralization is estimated at ca. 2700–2690 Ma (Davis and Smith 1991; Ayer and Dostal 2000).

Base metal deposits, characteristic of the centre–east areas (Long Bay – Manitou Lake), include the Wendigo mine (Cu–Au–Ag), which is largest past producer, and the nearby Maybrun (Cu–Au) and Kenbridge (Ni–Cu) properties, which are both potential producers (Davies 1973; Setterfield et al. 1983).

However, the dominant operating deposit in western Wabigoon subprovince lies at Sturgeon Lake, located 125 km east of Wabigoon Lake along the continuing greenstone belt extension. Sphalerite–chalcopyrite–pyrite-rich VMS deposits lie in felsic pyroclastic breccia dated at 2735 Ma, i.e., Lower Keewatin equivalent. Mattabi Mine, the largest of four such deposits, contains at least 11.4 million t of ore grading 0.7% Cu, 0.85% Pb, 8.28% Zn, and 104 g/t Ag (Franklin 1996).

Geochemistry and petrogenesis

In the Lake of the Woods area, assorted Upper Keewatin tholeiitic–calc-alkalic basalts and andesites (Fig. 7A: fields *I*, *II*) occur together with pyroclastic-rich andesites–dacites–rhyolites–shoshonites (Fig 7A: field *I*), the latter group characterized by "high La/Yb" trend and positive Eu anomalies. Those in the Long Bay – Kakagi Lake area include tholeiitic–calc-alkaline basalts and andesites (Fig. 7B: fields *II*, *III*), with modest mainly adakitic dacites (Fig. 7B: field *I*). Those in the Wabigoon–Manitou lakes area are of assorted mafic–felsic classes (Fig. 7B: fields *II*, *III*, *V*) that are classic calc-alkaline, with pronounced "high Yb" trend and negative Eu anomalies. In summary, this regional volcanic assemblage displays over a strike-length of 200 km a continuous intragreenstone belt that is a geochemical transition from adakitic in the west, through adakitic – classic calc-alkaline in the centre, to classic calc-alkaline in the east.

Ayer and Davis (1997) demonstrated that (1) Lower Keewatin tholeiites are similar to modern arc tholeiites at destructive margins, (2) Upper Keewatin calc-alkaline suite rocks are similar to calc-alkaline units forming in modern mature island-arc settings, and (3) electrum assemblage shoshonites are similar to modern shoshonites forming in late-stage development of mature island arcs at continental margins. Furthermore, Ayer and Davis (1997) and Ayer and Dostal (2000) attributed the derivation of Upper Keewatin tholeiitic and calc-alkaline suites, respectively, to separate mantle sources.

Ujike and Goodwin (2002) ascribed Upper Keewatin adakites to magmas produced by interaction of partial melts of subducted oceanic crust with a mantle wedge, and accompanying shoshonites to mantle peridotites similarly metasomatized by slab-derived adakitic melts.

Fig. 7. $(La/Yb)_N$ – $(Yb)_N$ plots of western Wabigoon region (western Wabigoon belt, Superior Province) volcanic samples by area. (A) Lake of the Woods area. (B) Long Bay – Kakagi Lake area. (C) Wabigoon–Manitou lakes area. Boundaries of fields *I–VI*, as in Fig. 5. Data used in Lesher et al. (1986); Ujike and Goodwin (2002). Inset map shows geological provinces of the Canadian Shield, including Slave and Superior provinces, and locations of western Wabigoon and Kirkland Lake – Noranda regions in Superior Province. Volcanic class symbols as in Fig. 3; alkaline suite, open triangle.

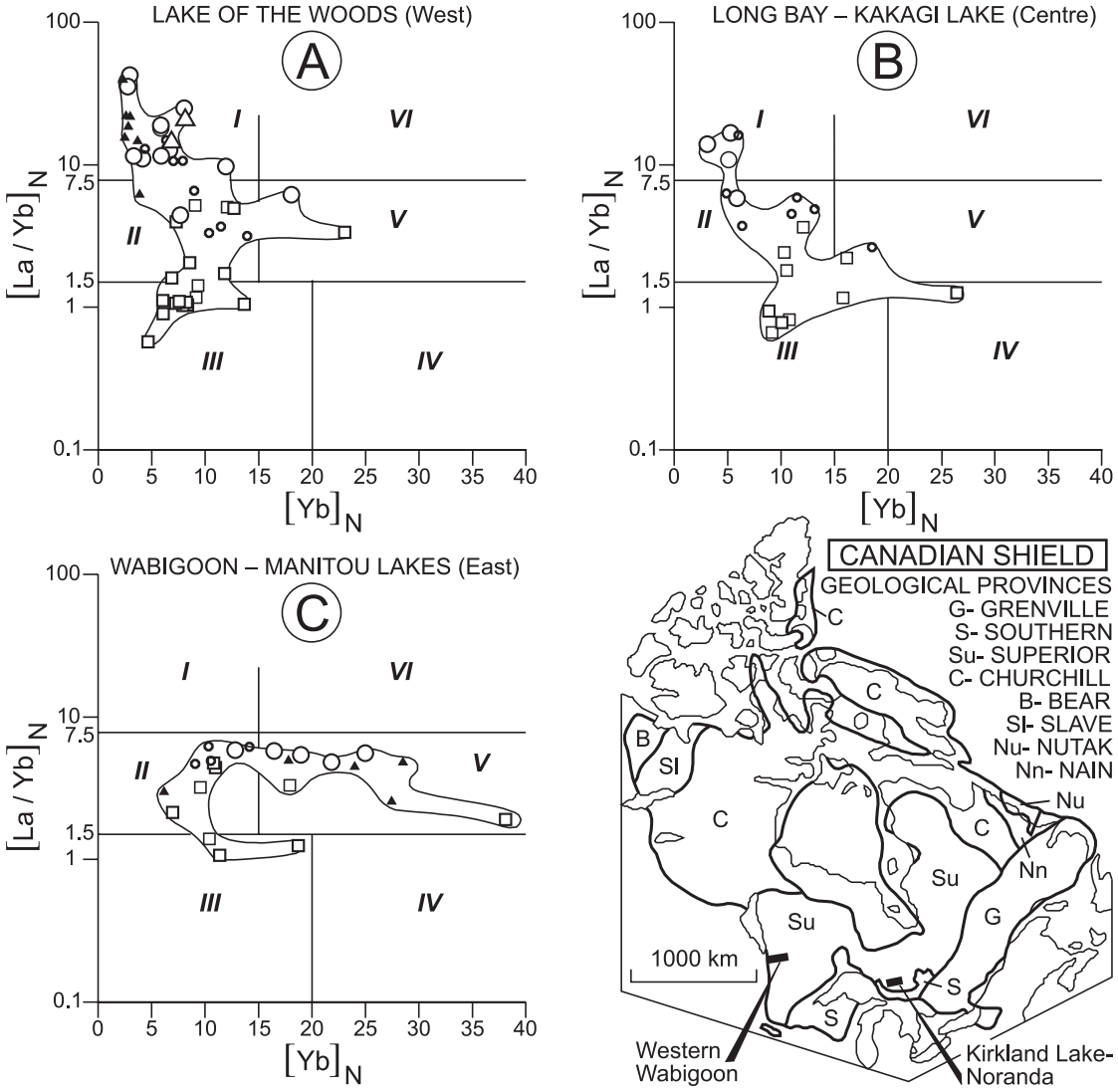

Kirkland Lake – Noranda region, south-central Abitibi belt, Superior Province

Belt setting and lithostratigraphy

This well-studied highly mineralized region (Fig. 7, inset map) (Goodwin 1979; de Rosen-Spence 1976; Spence and de Rosen-Spence 1975; Capdevila et al. 1982; Gelinas and Ludden 1984; Ujike 1985; Jackson and Fyon 1991; Fyon et al. 1991; Corfu 1993; Corfu et al. 1989, 1991; Ayer et al. 2002; Ayer et al. 2005) includes two separate late Neoarchean volcanic complexes located at Kirkland Lake and Noranda, which is120 km to the east–northeast. The two volcanic complexes are structurally separated by the east-trending Larder – Cadillac Break (ca. 2670 Ma), a major, craton-scale, south-side-up, multistage thrust fault of largely underdetermined net lateral and vertical displacements. For the most part, greenschist metamorphic grade prevails in the volcanic rocks.

The Kirkland Lake complex features a thick (up to 16 km), steeply dipping, outward-facing, homoclinal, volcanic succession that is exposed around the northern and eastern margins of the Round Lake batholith (2700–2697 Ma). This volcanic assemblage (Fig. 8A) is mainly divided into the lower, tholeiitic basalt-dominated Catharine Group (2725–2720 Ma) and the conformably overlying, pyroclastic-rich, adakitic-bearing Skead Group (2701–2697 Ma). Nearby to the north is the unconformably overlying, highly deformed, east-trending, south-dipping and facing Timiskaming Group (2676–2670 Ma), which is a distinctive conglomerate–sandstone assemblage, with prominent alkaline magmatic (trachyte–syenite) associates. The Timiskaming Group, which is bounded to the south mainly by the Larder – Cadillac Break and to

Fig. 8. $(La/Yb)_N$ – $(Yb)_N$ plots of southern Abitibi belt volcanic samples. (A) Kirkland Lake area: Catharine and Skead groups, and Timiskaming Group samples. (B) Central Noranda area: Noranda subgroup, and Blake River Group samples. Boundaries of fields *I–VI* as in Fig. 5. Data used in Capdevila et al. (1982); Lesher et al. (1986); Ujike and Goodwin (1987). Volcanic class symbols as in Fig. 7.

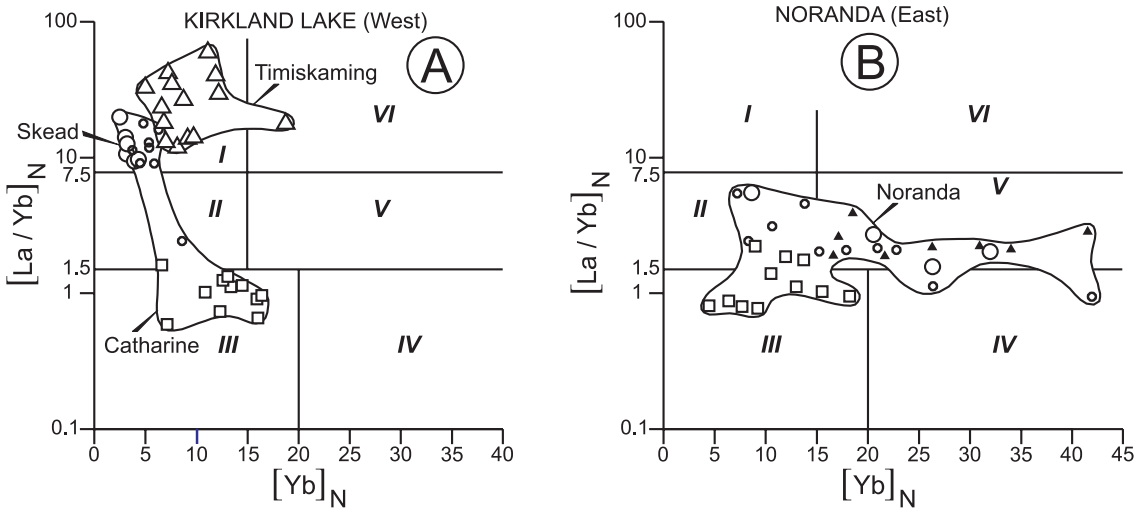

the north by the east-trending Blake River Group (2701–2697 Ma), i.e., coeval with the Skead Group of Kirkland Lake complex, is a 13.5 km thick, major regional volcanic assemblage (Baragar 1968) that continues eastward to the central Noranda area and beyond.

The central Noranda area, some 200 km^2 in size, lies immediately north of the town of Rouyn-Noranda. The area is underlain mainly by a 5 km thick cyclical sequence of mostly pillowed subaqueous andesite and heterogeneous rhyolite lava flows that are part of the upper Noranda subgroup of the Blake River Group. This assemblage is regionally deformed about an east-trending and plunging regional anticlinorial axis, resulting in gently east-trending open folds (de Rosen-Spence 1976). The underlying parts of the group, exposed within adjoining regional synclinoria to the north and south, include substantial komatiitic–tholeiitic components. Granitoid intrusions are common.

Mineralization

The region is notable for spectacular mineralization, which is characterized by world-class (1) epigenetic lode gold at Kirkland Lake and (2) syngenetic base-metal VMS at Noranda. The two contrasting metal deposit types are by no means mutually exclusive but commonly co-occur at lower grades.

Kirkland–Larder lakes lode-gold deposits have collectively produced a remarkable >1000 t Au (Jackson and Fyon 1991). Most deposits are related to quartz veins, sulphide-rich envelopes, and carbonate-altered rocks within late-stage shear zones of both the Main Break (Kirkland Lake) and nearby Larder–Cadillac (Larder Lake) Break. Major gold deposition occurred ca. 2673–2580 Ma (Fyon et al. 1991), i.e., immediately post-Timiskaming.

In sharp contrast, the central Noranda base-metal VMS deposits mainly represent syngenetic accumulates in a large central volcano setting. The area has produced a remarkable > 90 million t of Cu–Zn ore with variable Au/Ag (Franklin 1996). At least 12 base-metal VMS deposits are clustered within the upper Blake River Group; each deposit is rooted by stringers in chloritic–sericitic alteration pipes. The ore deposits are attributed to contemporaneous deposition on the sea floor as hard sinter over hot-spring orifices (Spence and de Rosen-Spence 1975), especially during or following periods of cauldron collapse (Fyon et al. 1991). Additional gold-bearing quartz veins occur nearby (Franklin 1996).

Geochemistry and petrogenesis

In the Kirkland Lake complex, Skead Group pyroclastic-rich, adakitic andesites and dacites are characterized by "high La/Yb" trend and positive Eu anomalies, as are (and even more so) the unconformably overlying Timiskaming alkalic rocks (Fig. 8A: field *I*). These assemblages overlie the older tholeiitic-rich Catharine assemblage (Fig. 8A: fields *II*, *III*). It is noted that alkalic-bearing Timiskaming-type sedimentary deposits, which are evidence of "pull-apart" basin deposition, are broadly distributed across Superior Province (Jirsa 2000). In sharp contrast, in the central Noranda area (Fig. 8B), basalt–andesite–dacite–rhyolite rocks of the upper Blake River Group (mainly Noranda subgroup) provide the archetypal, classic calc-alkaline, "high Yb" trend, together with pronounced negative Eu anomalies.

Corfu (1993) attributed southern Abitibi greenstone belt development to an oceanic setting by processes controlled by plate convergence and subduction. Ayer et al. (2002) emphasized that new mapping and U–Pb zircon geochronology results in the southern Abitibi greenstone belt, notably the presence of widespread contained inherited zircons with ages similar to those found in underlying assemblages, support an autochthonous regional volcanic construction rather than a collage of previously allochthonous terranes. Ujike and Goodwin (2002) attributed the archetypal Timiskaming alkaline magmatism to partial melting of mantle sources previously (20–30 million years) enriched by adakitic volcanism of the Skead Group.

Comparison of Slave Province and Superior Province

The salient points of comparison between Slave and Superior provinces are as follows: (1) Slave Province, at $190 \times l0^3$ km^2, is one-eight the size of Superior Province and contains generally smaller greenstone belts; (2) Yellowknife Supergroup has an unusually high ratio of sedimentary:volcanic rocks; (3) Slave Province Archean terrains feature widespread exposure and proximity of gneiss–migmatite basement that, together with unconformably overlying younger felsic volcanic edifices, provided ready epiclastic sources for the widespread metasediments (Jenner et al. 1981); (4) Slave Province greenstone terrains reveal much evidence in favour of early-stage expansion tectonics in both the basement and lowermost cover sequences, succeeded by later-stage convergence; and (5) Slave Province greenstones have comparatively few ultramafic komatiites in lower stratigraphic parts and few, if any, alkaline components, i.e., shoshonites–trachyte, in upper stratigraphic parts. Collectively in Slave Province, this may reflect (1) comparatively cool, early-stage mantle–plume activity resulting in smaller, thinner, ultramafic–alkaline deficient greenstone belts; and (2) comparatively shallow, hence lower pressure, alkaline-inhibiting, primary magma development at later stages.

However, despite these points of contrast, overall Slave and Superior late Neoarchean greenstone belt style and composition correspond closely. Although the relative positions of the two evolving cratons in late Archean time are unknown, their similarities point to similar or common mantle sources and petrogenetic processes. Both include prolific mesothermal lode-gold deposits in sheared and altered host rocks (2.73–2.60 Ga) (Bleeker 2002). A further overriding similarity is the terminal granite "bloom" (ca.2.60–2.58 Ga), with consequent widespread stabilization of Archean crust (ca. 2.65–2.55 Ga). This event was possibly facilitated by some deepening subduction-induced phase change (at ca. 50–80 km), such as the spinel–garnet transition (Watson and McKenzie 1991) or related eclogitization (Bjornerud and Austrheim 2004). The ensuing crustal stabilization is evidenced by subsequent first-order crustal events: (1) craton-scale strike–slip-dominated faults, e.g., Beaulieu River fault zone (ca. 2.68–2.55 Ga); (2) giant radiating dyke swarms, e.g., Matachewan swarm (2.48– 2.44Ga); and (3) The first modern-style, sediment-rich, passive margin sequences, e.g., Huronian Supergroup, at the southern margin of the Superior craton (2.48–2.2 Ga) (Bleeker 2002).

Volcano-metallogenic considerations

Base metal sulphides

Late Neoarchean felsic metavolcanic rocks (>64% $Si0_2$) in Superior Province have been divided into three main groups on the basis of trace element abundances and ratios (Lesher et al. 1986; Condie 1976; Barrie et al. 1993). Following Lesher et al. (1986) (further characterized in Fig. 6), field I group volcanic sequences, since recognized as typically adakitic, lack associated base-metal VMS deposits; in sharp contrast, field III group, which is of typical classic calc-alkaline composition, commonly hosts large important VMS deposits.

Barrie et al. (1993) noted that the VMS deposits associated with the then-designated field III group, but now designated as classic calc-alkaline volcanic sequences, are commonly underlain by large, high-level, cogenetic, synvolcanic intrusions that were capable during crystallization and cooling of providing the heat necessary to drive hydrothermal convective cells, which, given reasonable permeability and temperature constraints (Campbell et al. 1981), could leach metals from the volcanic pile and precipitate them on the paleosea floor. As an alternative mechanism, Yang and Scott (2002) hypothesized that felsic magmas, by degassing metal-rich magmatic fluids, directly contributed large quantities of ore metals directly to the formation of sea-floor and sub-sea-floor VMS deposits, as well as provided heat to drive the hydrothermal convection.

Lode-gold deposits

The genesis of Canadian Shield lode-gold deposits remains the subject of much debate (Robert 1996). A favoured model involves the circulation of meteoric waters during accretionary tectonic processes; previously dispersed gold is leached by upward-chanelling fluids along crustal-scale faults for eventual lode-gold deposition (Robert 1996; Kerrich 1990; Wyman et al. 1999). Such models thereby allow for late-stage concentration of previously dispersed gold in favourable structural sites.

Thus, the prolific, shield-wide, late Neoarchean (2.73–2.60 Ga), mesothermal, lode-gold deposition may have formed in response to late-stage, plate-tectonic-style, acretionary–collisional events during the tectonic aggregation of previously smaller dispersed sialic nuclei to form larger amalgamated more stable sialic cratons. This major sialic-craton-building tectonic process stimulated circulation of large volumes of deep distal auriferous fluids (Sener et al. 2005). During this particular late-Neoarchean tectonic cycle, the resulting greenstone lode-gold enrichment preferentially favoured the deeper sourced, thicker, more structurally active, adakitic volcanic complexes compared with nearby, thinner, shallower sourced, structurally benign, normal calc-alkaline volcanic counterparts.

Proposed metallotectonic model

Proposed tectonic origins for the Slave Province greenstone belts include (1) island arcs (Folinsbee et al. 1968); (2) slivers of ocean crust trapped between colliding cratons (Kusky 1989, 1990); (3) back-arc basins intruded and overlain by later arc volcanism (Helmstaedt and Padgham 1986); (4) continental rifts (Henderson 1985); and (5) marginal continental-rift setting (Bleeker et al. 1999*a*, 1999*b*; Bleeker 2002; Cousens 2000).

Salient aspects of Archean greenstone belt development include (1) greenstone assemblages are commonly deposited on TTG basement; (2) depositional contact commonly begins with thin micaceous quartzite and (or) thin chert and BIF; (3) above this are thick lower successions of tholeiitic mafic – subordinate ultramafic submarine lavas, with conformably overlying calc-alkaline, intermediate–felsic-bearing, volcanic sequences, both often in repeated cycles; (4) widespread diapiric granitoid intrusions, concurrently following felsic volcanic accumulation, form patterns of domal batholiths separated by synclinally sinuous greenstone networks; and

(5) later epiclastic sediments, variably eroded from basement gneisses, batholiths and felsic volcanic sources, cover the older volcanic units.

On the one hand, Hamilton (1998, 2003) and Bleeker (2002), among others, have marshalled salient criteria against the operation of modern-style, subduction-driven, plate tectonics in the development of Archean greenstone belts. Included are (1) the belts are commonly deposited on, or near, granitoid basement; (2) the resulting belts display essential autochthonous–parautochthonous tectono-stratigraphic relations, despite pervasive domal intrusion and structural deformation; and (3) Archean greenstone assemblages display few, if any, of the many identifiable stratigraphic, structural, and petrologic indicators of rifting, stratal-wedge deposition, oceanic separation, subduction, and collision that characterize plate-tectonic interactions of later times. However, plate-tectonic rifting and convergence were operating at least by ca. 2.0 Ga and were in essentially modern mode by ca. 0.8 Ga (Hamilton 1998).

On the other hand, the geochemical data from the late Neoarchean TTG–greenstone analogues, extensively cited earlier in the text, favour a subduction-involved, tectonic process. Pertinent considerations include (1) The chemical composition of TTG magmas evolved across Archean time (4.0–2.5 Ga) in response to progressively increasing pressures at the site of slab melting and the correspondingly increasing interaction of TTG magmas with mantle peridotite (Martin et al. 2005). In brief, such interactions were rare to absent in early Archean time (4.0–3.0 Ga), but widespread in late Archean time (3.0–2.5 Ga), where the development of a thick overlying mantle wedge ensured interaction between the slab-melts and mantle peridotite. (2) Subtle, widely repeated, late Neoarchean adakitic versus classic calc-alkaline greenstone dualities, each with distinctive metallotectonics, suggest that the existing lithosphere was sufficiently cool and dense to accommodate subduction down to variably modest micro-depths, say in the order of 50–150 km.

The challenge, then, is to propose a model that allows for the appropriate slab-melt–mantle interactions, yet results in essentially autochthonous (i.e., in situ) greenstone belt development. This seeming dilemma can be resolved by invoking the operation of late Neoarchean, entry-level, microplate tectonics—a paradigm shift in operation of Earth's progressively cooling, hence deepening subduction-accommodating mantle, as considered further later in the text.

On the one hand, modern plate tectonics involves geographically long, structurally complex and sophisticated, circum-oceanic island-arc systems, operating in relation to large stable continents. Current subduction zones extend to depths of ca. 7000 km (Hamilton 2003, Fig. 7); this provides the measure of existing, cool, brittle lithosphere. Archean tectonic processes, on the other hand, operated in an evolving thermal regime in which the average upper mantle temperature was up to 200–300 °C hotter and the heat flux two to three times greater than at present (Rapp et al. 1991). In such an environment, the inferred late Neoarchean microplate tectonics involved ocean-type mafic crust with accompanying small unstable sialic nuclei of lateral dimensions to be measured in tens to several hundred kilometres, i.e., orders of magnitude smaller than present-day continents. The proposed small-scale, high-temperature, fast-moving, shallow subduction-driven tectonic process was tightly compressed in space and time; it produced small arc-type volcanic sequences commensurate in size with adjoining sialic cratons. Resulting regional supracrustal assemblages, despite pervasive structural and intrusive distortions, retain, on the one hand, persuasive chemical evidence of slab-melt–mantle interactions, yet on the other hand, essential in situ tectono-stratigraphic relations.

In summary, the southern Slave Province region (Fig. 6) includes a two-fold association: (1) in the east, the stratigraphically thin, moderately folded, rhyolite-rich, classic calc-alkaline flow assemblage, together with syngenetic VMS deposits, is attributed to fractionation processes initiated at comparatively shallow depths, leading to substantial magma fractionation in shallow-level magma chambers, during comparatively slow magma ascent to surface; and (2) in the west, the stratigraphically thick, structurally complex, rhyolite-poor, pyroclastic-rich, adakitic-bearing, volcanic assemblage, together with late-stage, mesothermal lode-gold deposits, in turn attributed to fractionation processes initiated at greater depths, followed by comparatively rapid magma ascent, with resulting explosive-rich extrusion and the deposition of gold as a product of late-stage collisional events. In brief, this regional volcano-metallotectonic duality is tentatively attributed to a shallow, westerly inclined (present geography) subduction zone(s), which produced, in the east, the shallower derived, stratigraphically simple, classic calc-alkaline, arc-type, flow-rich assemblage with VMS associates, and, in the west, the deeper derived, stratigraphically complex, structurally deformed, adakitic, back-arc basin-type assemblage with late-stage lode-gold associates. In both cases, the formative magmatic processes involved substantial crustal assimilation (Fig. 5).

In the larger context, following end-Archean time, itself marked by widespread, TTG-bloom-induced, craton growth and stability, Earth's cooling mantle, with progressively (1) deepening subduction, (2) growing tectonic plates, (3) enlarged and stabilized cratons, and (4) appropriate metallogenic response, continued unabated across ensuing Proterozoic time and beyond, into the operation of modern-mode plate tectonics.

Further studies in a broader range of late Neoarchean greenstone belts are required to (1) test the validity of the proposed volcano-metallotectonic model, and (2) better define the critical primary, three-dimensional, synvolcanic relations in the growing assemblages that were parent to the now structurally reoriented, mutually displaced, volcanic complexes within the preserved greenstone belts.

Acknowledgments

We gratefully acknowledge the constructive criticism and helpful advice given by K.M. Ansdell, J.A Ayer, W. Bleeker, A. Polat, and unnamed reviewer. We thank M.P. Gorton for his help with X-ray fluorescence analyses, and the Natural Sciences and Engineering Council for financial support. Subhash Shanbhag and Karyn Gorra, Department of Geology, University of Toronto, Toronto, Ontario, respectively provided expert art and photographic work.

References

Atkinson, D. 1990. Archean polymetallic volcanogenic massive sulphide deposits within the Cameron and Beaulieu River volcanic belts. 8th IAGOD (International Association on the Genesis of Ore Deposits) Symposium. Field Trip Guidebook. Geological Survey Canada, Open File 2168, pp. 99–108.

Ayer, J.A., and Davis, D.W. 1997. Neoarchean evolution of differing convergent margin assemblages in the Wabigoon Subprovince: geochemical and geochronological evidence from the Lake of the Woods greenstone belt, Superior Province, Northwestern Ontario. Precambrian Research, **81**: 155–178.

Ayer, J.A., and Dostal, J. 2000. Nd and Pb isotopes from the Lake of the Woods greenstone belt, northwestern Ontario: implications for mantle evolution and the formation of crust in the southern Superior Province. Canadian Journal of Earth Science, **37**: 1677–1689.

Ayer, J., Amelin,Y., Corfu, F., Kamo, S., Ketchum, J., Kwok, K., and Trowell, N. 2002. Evolution of the southern Abitibi greenstone belt based on U–Pb geochronology: autochthonos volcanic construction followed by plutonism, regional deformation and sedimentation. Precambrian Research, **115**: 63–95.

Ayer, J.A., Thurston, P.C., Bateman, R., Dubé, B., Gibson, H.L., Hamilton, M.A. et al. 2005. Overview of results of the Greenstone Architecture Project: Discover Abitibi Initiative. Ontario Geological Survey, Open File Report 6154.

Baragar, W.R.A. 1966. Geochemistry of the Yellowknife volcanic rocks. Canadian Journal Earth Sciences, **3**: 9–30.

Baragar, W.R.A. 1968. Major-element geochemistry of the Noranda volcanic belt, Quebec–Ontario. Canadian Journal of Earth Sciences, **5**: 773–790.

Barnes, S.J., and Gorton, M.P. 1984. Trace element analysis by neutron activation with a low flux reactor (SLOWPOKE II): results for international standards. Geostandards Newsletter, **8**(1): 17–23.

Barrie, C.T. 1995. Zircon thermometry of high-temperature rhyolites near volcanic-associated massive sulfide deposits, Abitibi subprovince, Canada. Geology, **23**: 169–172.

Barrie, C.T., Ludden, J.N., and Green, T.H. 1993. Geochemistry of volcanic rocks associated with Cu–Zn and Ni–Cu deposits in the Abitibi subprovince. Economic Geology, **88**: 1341–1358.

Bjornerud, M.G., and Austrheim, H. 2004. Inhibited eclogite formation: The key to the rapid growth of strong and buoyant Archean continental crust. Geology, **32**: 765–768.

Blackburn, C.E., Johns, G.W., Ayer, J., and Davis, D.W. 1991. Wabigoon Subprovince. *In* Geology of Ontario. Special Vol. 4, Part 1. Ontario Geological Survey, pp. 303–381.

Bleeker, W. 2001. The ca. 2680 Ma Raquette Lake Formation and correlative units across the Slave Province, Northwest Territories: evidence for a craton-scale overlap sequence. *In* Current research. Geological Survey of Canada, Paper 2001-C7, 26 p.

Bleeker, W. 2002. Archean tectonics—a review, with illustrations from the slave craton. The early Earth: physical, chemical and biological development. *Edited by* C.M.R. Fowler, C.J. Ebinger, and C.J. Hawkesworth. Geological Society (of London), Special Publication 199, pp. 151–181.

Bleeker, W., Ketchum, J.W.F., Jackson, V.A., and Villeneuve, M.E. 1999*a*. The Central Slave Basement Complex, Part 1: its structural topology and autochthonous cover. Canadian Journal of Earth Sciences, **36**: 1083–1109.

Bleeker, W., Ketchum, J.W.F., and Davis, W.J. 1999*b*. The Central Slave Basement Complex, Part II: age and tectonic significance of high-strain zones along the basement–cover contacts. Canadian Journal of Earth Sciences, **36**: 1111–1130.

Bleeker, W., Stern, R., and Sircombe, K. 2000. Why the Slave Province, Northwest Territories, got a little bigger. *In* Current research. Geological Survey of Canada, Paper 2000-C2, 9 p.

Boily, M., and Dion, C. 2002. Geochemisty of boninite-type volcanic rocks in the Frotet-Evans greenstone belt, opatica subprovince: implications for the evolution of Archean greenstone belts. Precambrian Research, **115**: 349–371.

Bowring, S., and Housh, T. 1995. The Earth's early evolution. Science, **269**: 1535–1540.

Boyle, R.W. 1953. Mineralisation of the Yellowknife greenstone belt, with special reference to the factors which controlled its localization. Unpublished Ph.D. thesis, University of Toronto, Toronto, Ont.

Campbell, I.H., Franklin, J.M., Gorton, M.P., and Hart, T.R. 1981. The role of subvolcanic sills in the generation of massive sulfide deposits. Economic Geology, **76**: 2248–2253.

Capdevila, R., Goodwin, A.M., Ujike, O., and Gorton, M.P. 1982. Trace-element geochemistry of Archean volcanic rocks and crustal growth in southwestern Abitibi Belt, Canada. Geology, **10**: 418–422.

Condie, K.C. 1976. Trace-element geochemistry of Archean greenstone belts. Earth-Science Reviews, **12**: 393–417.

Condie, K.C., and Baragar, W.R.A. 1974. Rare-earth element distributions in volcanic rocks from Archean greenstone belts. Contributions to Mineral and Petrology, **45**: 237–246.

Corfu, F. 1993. The evolution of the southern Abitibi greenstone belt in light of precise U–Pb geochronology. Economic Geology, **88**: 1323–1340.

Corfu, F., Krogh, T.E., Kwok, Y.Y., and Jensen, L.S. 1989. U–Pb zircon geochronology in the southwestern Abitibi greenstone belt, Superior Province. Canadian Journal of Earth Sciences, **26**: 1747–1763.

Corfu, F., Jackson, S.L., and Sutcliffe, R.H. 1991. U–Pb ages and tectonic significance of late Archean alkalic magmatism and nonmarine sedimentation: Timiskaming Group, southern Abitibi belt, Ontario. Canadian Journal of Earth Sciences, **28**: 489–503.

Cousens, B.L. 2000. Geochemistry of the Archean Kam Group, Yellowknife Greenstone Belt, Slave Province, Canada. Journal of Geology, **108**: 181–197.

Cousens, B., Facey, K., and Falck, H. 2002. Geochemistry of the late Archean Banting Group, Yellowknife greenstone belt, Slave Province, Canada: simultaneous melting of the upper mantle and juvenile mafic crust. Canadian Journal of Earth Sciences, **39**: 1635–1656.

Daigneault, R., Mueller, W.U., and Chown, E.H. 2004. Abitibi greenstone belt plate tectonics: diachronous history of arc development, accretion and collision. *In* The Precambrian Earth: tempos and events. *Edited by* P.G. Eriksson, W. Altermann, D.R. Nelson, W.U. Mueller, and O. Catuneau. Elsevier, Amsterdam, The Netherlands, pp. 88–103.

Davies, J.C. 1973. Geology of the Atikwa Lake area, District of Kenora. Geological Report III, Ontario Division of Mines, Toronto, Ont.

Davis, D.W., and Smith, P.M. 1991. Archean gold mineralization in the Wabigoon subprovince, a product of crustal accretion: evidence from U–Pb geochronology in the Lake of the Woods area, Superior Province, Canada. Journal of Geology, **99**: 337–353.

Davis, D.W., Sutcliffe, R.H., and Trowell, N.F. 1988. Geochronological constraints on the tectonic evolution of a late Archean greenstone belt, Wabigoon subprovince, northwest Ontario, Canada. Precambrian Research, **39**: 171–191.

Davis, W.J., and Bleeker, W. 1999. Timing of plutonism, deformation, and metamorphism in the Yellowknife Domain, Slave Province, Canada. Canadian Journal of Earth Sciences, **36**: 1169–1187.

Davis, W.J., King, J.E., and Fryer, B.J. 1994. Geochemistry and evolution of Late Archean plutonism and its significance to the tectonic development of the Slave craton. Precambrian Research, **67**: 207–241.

de Rosen-Spence, A.F. 1976. Stratigraphy, development and petrogenesis of the Central Noranda volcanic pile, Noranda, Quebec. Unpublished Ph.D. thesis, University of Toronto, Toronto, Ont.

Defant, M.J., and Drummond, M.S. 1990. Derivation of some modern arc magmas by melting of young subducted lithosphere. Nature, **347**: 662–665.

Defant, M.J., and Kepezhinskas, P. 2001. Evidence of slab melting in arc magmas. EOS, Transactions of the American Geophysical Union, **82**: 65, 68–69.

Dostal, J., and Corcoran, P.L. 1998. Evolution of the Slave Province as recorded by physical volcanology, trace elements and isotopic systematics of selected Archean Greenstone belts along the Beniah Lake Fault Zone, Slave Province, Northwest Territories. Department of Indian Affairs and Northern Development, Northwest Territories Geology Division, Yellowknife, Economic Geology Series (EGS), Open File 1998-11.

Drury, S.A. 1983. The petrogenesis and setting of Archean metavolcanics from Karnataka State, South India. Geochimica et Cosmochimica Acta, **47**: 317–329.

Folinsbee, R.E., Baadsgaard, H., Cumming, G.L., and Green, D.C. 1968. A very ancient island arc. *In* The crust and upper mantle of the Pacific area. *Edited by* L. Knopoff, C.L. Drake, and P.J. Hart. American Geophysical Union, Geophysical Monograph, pp. 441–448.

Franklin, J.M. 1996. Volcanic-associated massive sulphide base metals. *In* Geology of Canadian mineral deposit types. *Edited by* O.R. Eckstrand, W.D. Sinclair, and R.I. Thorpe. Geological Survey of Canada, Geology of Canada, no. 8, pp. 158–183.

Fyon, J.A., Breaks, F.W., Heather, K.B., Jackson, S.L., Muir, T.L., Stott, G.M. et al. 1991. Metallogeny of metallic mineral deposits in the Superior Province of Ontario. *In* Geology of Ontario. Special Vol. 4, Part. 2. Ontario Geological Survey, pp. 1091–1174.

Garrison, J.M., and Davidson, J.P. 2003. Dubious case for slab melting in the Northern volcanic zone of the Andes. Geology, **6**: 565–568.

Gelinas, L., and Ludden, J.N. 1984. Rhyolitic volcanism and the geochemical evolution of an Archean central ring complex: the Blake River Group volcanics of the southern Abitibi belt, Superior province. Physics of the Earth and Planetary Interiors, **35**: 77–88.

Glikson, A.Y. 1976. Trace element geochemistry and origin of early Precambrian acid igneous series, Barberton Mountain Land, Transvaal. Geochimica et Cosmochimica Acta, **40**: 1261–1280.

Goodwin, A.M. 1965. Preliminary report on volcanism and mineralization in the Lake of Woods-Manitou Lake – Wabigoon region of NW Ontario. Ontario Department of Mines, PR 1965-2.

Goodwin, A.M. 1977. Archean volcanism in Superior Province, Canadian Shield. *In* Volcanic regimes in Canada. *Edited by* W.R.A. Baragar, L.C. Coleman, and J.M. Hall. The Geological Association of Canada, Special Paper 16, pp. 205–244.

Goodwin, A.M. 1979. Archean volcanic studies in the Timmins – Kirkland Lake – Noranda region of Ontario and Quebec. Geological Survey of Canada, Bulletin 278.

Goodwin, A.M. 1988. Geochemistry of Slave Province volcanic rock: Yellowknife belt. *In* Contributions to the geology of the Northwest Territories. Vol. 3. Indian and Northern Affairs Canada (INAC), Northwest Territories Geology Division, Yellowknife, Northwest Territories, pp. 13–25.

Hamilton, W.B. 1998. Archean tectonics and magmatism. International Geology Review, **40**: 1–39.

Hamilton, W.B. 2003. An alternative Earth. GSA Today, **13**(11): 4–12.

Hart, T.R., Gibson, H.L., and Lesher, M. 2004. Trace element geochemistry and petrogenesis of felsic volcanic rocks associated with volcanogenic massive Cu–Zn–Pb sulfide deposits. Economic Geology, **99**: 1003–1013.

Helmstaedt, H., and Padgham, W.A. 1986. A new look at the stratigraphy of the Yellowknife Supergroup at Yellowknife, N.W.T.—implications for the age of gold-bearing shear zones and Archean basin evolution. Canadian Journal of Earth Sciences, **23**: 454–475.

Henderson, J.B. 1970. Stratigraphy of the Archean Yellowknife supergroup; Yellowknife Bay – Prosperous Lake area, District of Mackenzie. Geological Survey of Canada, Paper 70-26.

Henderson, J.B. 1985. Geology of the Yellowknife – Hearne Lake area, District of Mackenzie: a segment across an Archean basin. Geological Survey of Canada, Memoir 414.

Henderson, J.B., vau Breeman, O., and Loveridge, W.D. 1987. Some U–Pb zircon ages from Archeau basement, supracrustal and intrusive rocks, Yellowknife – Hearne Lake area, District of Mackenzie. *In* Ragiogenic age and isotope studies. Geological Survey of Canada, Paper 87-2, pp. 111–121.

Isachsen, C.E. 1992. U–Pb zircon geochronology of the Yelloknife volcanic belt and subjacent rocks, N.W.T., Canada: Constraints on the timing, duration, and mechanics of greenstone belt formation. Ph.D. thesis, Washington University, St. Louis, Mo. (cited in Cousens et al. 2002).

Isachsen, C.E., and Bowring, S.A. 1994. Evolution of the Slave craton. Geology, **22**: 917–920.

Isachsen, C.E., and Bowring, S.A. 1997. The Bell Lake group and Anton Complex: a basement–cover sequence beneath the Archean Yellowknife greenstone belt revealed and implicated in greenstone belt formation. Canadian Journal of Earth Sciences, **34**: 169–180.

Jackson, S.L., and Fyon, J.A. 1991. The western Abitibi subprovince in Ontario. *In* Geology of Ontario. Vol. 4, Part 1. Ontario Geological Survey, pp. 405–482.

Jahn, B.-M., Glikson, A.Y., Peucat, J.J., and Hickman, A.H. 1981. REE geochemistry and isotpic data of Archean silicic volcanics and granitoids from the Pilbara Block, Western Australia: implications for the early crustal evolution. Geochimica et Cosmochimica Acta, **45**: 1633–1652.

Jenner, G.A., Fryer, B.J., and McLennan, S.M. 1981. Geochemistry of the Archean Yellowknife Supergroup. Geochimica et Cosmochimica Acta, **45**: 1111–1129.

Jirsa, M.A. 2000. The Midway sequence: a Timiskaming pull-apart basin deposit in western Wawa subprovince, Minnesota. Canadian Journal Earth Sciences, **37**: 1–15.

Kerrich, R. 1990. Mesothermal gold deposits: a critique of genetic hypotheses. *In* Greenstone gold deposits. Geological Association of Canada, Nuna Conference Vol., pp. 13–31.

Ketchum, J.W.F., Bleeker, W., Stern, R.A., 2004. Evolution of an Archean basement complex and its antochthonous cover, southern Slave Province, Canada. Precambrian Research, **135**: 149–176.

Kusky, T.M. 1989. Accretion of the Archean Slave province. Geology, **17**: 63–67.

Kusky, T.M. 1990. Evidence for Archean ocean opening and closing in southern Slave province. Tectonics, **9**: 1533–1563.

Lambert, M.B. 1977. Anatomy of a greenstone belt-Slave province, N.W.T. *In* Volcanic regimes in Canada. *Edited by* W.R.A. Baragar, L.C. Coleman, and J.M. Hall. Geological Association of Canada, Special Paper 16, pp. 331–340.

Lambert, M.B. 1988. Cameron River and Beaulieu River volcanic belts of the Archean Yellowknife Supergroup, District of Mackenzie,

Northwest Territories. Geological Survey of Canada, Bulletin 382, 145 p.

Lesher, C.M., Goodwin, A.M., Campbell, I.H., and Gorton, M.P. 1986. Trace-element geochemistry of ore-associated and barren, felsic metavolcanic rocks in the Superior Province, Canada. Canadian Journal Earth Sciences, **23**: 222–237.

Manikyamba, C., Nagvi, S.M., Rao, D.V.S., Mohan, M.R., Khanna, T.C., Rao, T.G. et al. 2005. Boninites from the Neoarchean Gadwal Greenstone belt, Eastern Dharwar Caton, India: implications for Archean subduction processes. Earth and Planetary Science Letters, **230**: 65–85.

Martel, E., Lin, S., and Bleeker, W. 2002. Kinematic observations in the Yellowknife River Fault Zone and structures in the Jackson Lake Formation, Yellowknife Greenstone Belt, Northwest Territories. *In* Current research. Geological Survey of Canada, Paper 2002-E4, pp. 1–10.

Martin, H. 1986. Effect of steeper Archean geothermal gradient on geochemistry of subduction-zone magmas. Geology, **14**: 753–756.

Martin, H. 1987. Petrogenesis of Archaen trondhjemites, tonalites and granodiorites from Eastern Finland: major and trace element geochemistry. Journal of Geology, **28**: 921–953.

Martin, H. 1999. Adakitic magmas: modern analogues of Archaean granitoids. Lithos, **46**: 411–429.

Martin, H., and Moyen, J.F. 2002. Secular changes in tonalite–trondhjemite–granodiorite (TTG) composition as markers of the progressive cooling of the Earth. Geology, **30**: 319–322.

Martin, H., Smithies, R.H., Rapp, R., Moyen, J-F, and Champion, D. 2005. An overview of adakite, tonalite–trondhjemite–granodiorite (TTG), and sanukitoid: relationships and some implications for crustal evolution. Lithos, **79**: 1–24.

Mueller, W.U., and Corcoran, P.L. 1997. Volcanology and sedimentology of the Raquette Lake Formation: a remnant dissected arc sequence. Indian and Northern Affairs, Yellowknife, Economic Geology Series (EGS), 1997-11.

Padgham, W.A. 1990. The Slave Province: an overview, in mineral deposits of the Slave Province. 8th IAGOD (International Association on the Genesis of Ore Deposits) Symposium. Field Trip Guidebook. Geological Survey Canada, Open File 2168, pp. 1–40.

Polat, A., and Kerrich, R. 2001. Magnesian andesites, Nb-enriched basalt-andesites, and adakites from late-Archean 2.7 Ga Wawa greenstone belts, Superior Province, Canada: implications for late Archean subduction zone petrogenetic processes. Contributions to Mineralogy and Petrology, **141**: 36–52.

Rapp, R.P., and Watson, E.B. 1995. Dehydration melting of metabasalt at 8–32 kbar: implications for continental growth and crust-mantle recycling. Journal of Petrology, **36**: 891–931.

Rapp, R.P., Watson, E.B., and Miller, C.F. 1991. Partial melting of amphibolite/eclogite and the origin of Archean trondhjemites and tonalites. Precambrian Research, **51**: 1–25.

Rapp, R.P., Shimizu, N., Norman, M.D., and Applegate, G.S. 1999. Reaction between slab-derived melts and peridotite in the mantle wedge: experimental constraints at 3.8 GPa. Chemical Geology, **160**: 335–356.

Robert, F. 1996. Quartz-carbonate vein gold. *In* Geology of Canadian mineral deposit types. *Edited by* O.R. Eckstrand, W.D. Sinclair, and R.I. Thorpe. Geological Survey of Canada, Geology of Canada, no. 8, pp. 350–366.

Samaniego, P., Martin, H., Robin, C., and Monzier, M. 2002. Transition from calc-alkalic to adakitic magmatism at Cayambe volcano, Ecuador: insights into slab melts and mantle–wedge interactions. Geology, **30**: 967–970.

Samsonov, A.V., Bogina, M.M., Bibikova, E.V., Petrova, A.Y., and Shchipamsky, A.A. 2005. The relationship between adakitic, calc-alkaline volcanic rocks and TTG: implications for the tectonic setting of the Kareliau greenstone belts, Baltic Shield. Lithos, **79**: 83–106.

Sener, A.K., Young, C., Groves, D.I., Krapež, B., and Fletcher, I.R., 2005. Major orogenic gold episode associated with Cordilleran–style tectonics related to the assembly of Paleoproterozoic Australia? Geology, **33**: 225–228.

Setterfield, T., Watkinson, D.H., and Thurston, P.C. 1983. Quench-textured, pillowed metabasalts and copper mineralization, Maybrum Mine, northwestern Ontario. Canadian Institute of Mining and Metallurgy, Bulletin 76, pp. 69–74.

Siddorn, J., and Cruden, S.A. 2000. Timing of mineralization in the Giant and Con gold deposits, Yellowknife, Canada. *In* 28th Yellowknife Geoscience Forum. Program and Abstracts. Indian and Northern Affairs Canada, Yellowknife, N.W.T., pp. 68–69.

Spence, C.D., and de Rosen-Spence, A.F. 1975. The place of sulfide mineralization in the volcanic sequence at Noranda, Quebec. Economic Geology, **70**: 90–101.

Taylor, S.R., and Gorton, M.P. 1977. Geochemical application of spark source mass spectrography-III. Element sensitivity, precision and accuracy. Geochimica et Cosmochimica Acta, **41**: 1375–1380.

Taylor, S.R., and Hallberg, J.A. 1977. Rare-earth elements in the Marda calc-alkaline suite: an Archean geochemical analogue of Andean-type volcanism. Geochimica et Cosmachimica Acta, **41**: 1125–1129.

Taylor, S.R., and McLennan, S.M. 1981. The composition and evolution of continental crust: rare earth element evidence from sedimentary rocks. Philosophical Transactions of the Royal Society of London, Series A, **301**: 381–399.

Taylor, S.R., and McLennan, S.M. 1985. The continental crust: its composition and evolution. An examination of the geochemical record preserved in sedimentary rocks. Blackwell Scientific Publications, Oxford, UK.

Thurston, P.C., Ayres, L.D., Edwards, G.R., Gelinas, L., Ludden, J.N., and Verpaelst, P. 1985. Archean bimodal volcanism. *In* Evolution of Archean supracrustal sequences. *Edited by* L.D. Ayres, P.C. Thurston, K.D. Card, and W. Weber. Geological Association of Canada, Special Paper 28, pp. 13–20.

Ujike, O. 1985. Geochemistry of Archean alkaline volcanic rocks from the Crystal Lake area, east of Kirkland Lake, Ontario, Canada. Earth and Planetary Science Letters, **73**: 333–344.

Ujike, O., and Goodwin, A.M. 1987. Geochemistry and origin of Archean felsic metavolcanic rocks, central Noranda area, Quebec, Canada. Canadian Journal of Earth Sciences, **24**: 2551–2567.

Ujike, O., and Goodwin, A.M. 2002. Geochemistry of shoshonites from the Upper Keewatin assemblage, western Wabigoon belt, Superior Province, Canada. Journal of Mineralogical and Petrological Sciences, **97**: 269–277.

Van Hees, E., Shelton, K., McMenamy, T., Ross, L., Cousens, B., Falck, H. et al. 1999. Metasedimentary influence on metavolcanic-rock-hosted greenstone gold deposits: geochemistry of the Giant mine, Yellowknife, N.W.T. Geology, **27**: 71–74.

Watson, S., and McKenzie, D. 1991. Melt generation by plumes: a study of Hawaiian volcanism. Journal of Petrology, **32**: 501–537.

Wyman, D.A., Kerrich, R., and Groves, D.I. 1999. Lode gold deposits and Archean mantle plume-island arc interaction, Abitibi subprovince, Canada. The Journal of Geology, **107**: 715–725.

Yang, K., and Scott, S.D. 2002. Magmatic degassing of volatiles and ore metals into a hydrothermal system on the modern sea floor of the eastern Manus back-arc basin, Western Pacific. Economic Geology, **97**: 1079–1100.

Yogodzinski, G.M., Lees, J.M., Churikova, T.G., Dorendorf, F., Wöerner, G., and Volynets, O.N. 2001. Geochemical evidence for the melting of subducting oceanic lithosphere at plate edges. Nature, **409**: 500–504.

Appendix A. Trace and minor element contents by individual sample

Trace and minor element compositions of 51 re-analyzed volcanic samples from the Cameron River – Beaulieu River area. Sample No., original field sample number (Figs 2, 3, 5, 7, 8); Field No., corresponding original field as located in Lambert (1988, figs. 2, 3). Volcanic (Volc.) class abbreviations as in Fig. 3.

Table A1. Cameron River subarea.

Sample No.:	1	2	3	4	5	6	7	8	9	10	11	12	13	14
Field No.:	386	390	392	402	407	406	425	424	377	415	379	414	432	566
Volc. class:	Bs	Bs-An	Bs	Bs	Bs	Bs	Bs	Bs-An	An	An	Dc	Ry	Bs	Bs
La (ppm)	3.6	12	4.7	3.9	3.4	2.9	4.3	3.5	22.1	22.5	46.1	12.7	35.3	7.9
Ce	8.8	24.6	9.7	9.8	7.6	9.1	13.7	10.2	48.3	54	92	26.6	97.1	25.8
Nd	5.54	16.1	6.07	7.72	5.84	5.16	7.67	5.92	26.44	17.79	20.72	9.35	37.29	15.17
Sm	2.2	5.11	2.19	2.67	2.31	2.15	2.83	2.52	6.51	4.96	6.32	3.77	12.43	4.89
Eu	0.88	1.37	0.72	3.83	0.76	0.75	3.84	0.64	1.57	3.93	3.85	0.38	3.76	1.56
Eu_N	12.2	19	10	53.1	10.5	10.4	53.1	8.9	21.8	54.4	53.3	5.2	52.1	21.6
Eu^*_N	11.3	26	12.2	13.2	11.4	11.7	15.2	11.8	28.5	22	27	18.4	52	23.5
Tb	0.54	1.23	0.7	0.62	0.51	0.62	0.81	0.48	1.01	0.79	0.91	0.82	1.63	1.02
Ho	1.24	1.13	2.29	1.82	1.39	1.06	1.19	1.09	1.71	1.27	0	0	2.08	1.27
Yb	2.46	3.75	2.03	2.71	2.93	2.42	2.71	2.61	4.57	3.25	2.48	3.43	4.09	2.19
Lu	0.4	0.58	0.34	0.4	0.43	0.37	0.42	0.41	0.65	0.5	0.34	0.55	0.62	0.33
ΣREE	25.66	65.87	28.74	33.47	25.17	24.53	34.47	27.37	112.86	108.99	172.72	57.6	194.3	60.13
Th	0.87	1.08	0.74	0.3	0.27	0.23	0.66	0.27	2.76	6.72	29.76	22.57	4.14	0.27
Hf	2.28	3.48	1.76	1.99	1.44	1.41	2.04	1.78	5.15	5.14	5.73	3.12	9.59	3.32
Ta	0.21	0.36	0.13	0.21	0.17	0.11	0.22	0.14	0.8	0.69	1.16	0.97	2.02	0.35
Ba	17.5	0.1	30.9	63.3	0.1	8.2	52.5	0.07	62.5	444.9	416.1	157.1	349.1	124.4
Sc	38.36	37.48	44.02	45.06	43.9	44.32	53.71	39.38	23.56	38.64	12.69	1.88	41.76	23.39
Co	46.31	33.3	47.28	49.06	50.86	50.76	80.31	42.1	31.98	45.14	15.47	0.95	72.51	50.9
Cr	203	52	320	194	111	112	212	178	166	168	53	2	55	207
Ni	100	26	99	80	77	81	107	97	59	93	20	1	69	165
V	261	339	230	277	254	254	292	251	164	168	90	3	443	251
Zr	74	138	64	68	63	58	75	72	218	130	200	75	204	126
Y	25	38	24	25	27	22	27	25	43	23	30	41	34	28
Sr	107	122	181	123	137	105	126	128	159	162	189	57	396	308
Rb	5	0	3	2	5	2	2	2	9	29	127	209	21	100
$(La/Yb)_N$	0.97	2.11	1.53	0.95	0.77	0.79	1.05	0.89	3.19	4.57	12.27	2.45	5.7	2.38
$(Yb)_N$	25.66	18	9.76	13	14.1	11.6	7.07	12.52	21.97	15.6	11.9	16.5	10.67	5.72

Table A2. Tumpline Lake subarea.

Sample No.:	1	2	3	4	5	6	7	8	9	10	11	12	13
Field No.:	396	395	568	567	572	565	564	563	561	393	378	560	559
Volc. Class:	Bs-An	Bs	An	Dc	Ry	Ry	Ry	Ry	Ry	Ry	Ry	Ry	Ry
La (ppm)	9.3	15.3	25.7	31.2	72.9	50.4	34.7	50	49.2	55.6	24.7	59.8	48.5
Ce	24.7	33.2	68	67.3	127.3	97.3	72	101.8	87.5	108.5	60.3	117.4	96.4
Nd	8.36	18.4	25.81	26.05	46.53	44.37	26.81	34.33	34.09	31.35	18.47	33.54	37.72
Sm	3.04	4.4	6.96	7.55	10.43	9.45	6.98	8.59	8.89	9.79	6.09	8.93	7.51
Eu	0.99	1.29	3.65	1.46	0.79	1.4	0.97	0.65	0.99	1.18	1.81	1.04	3.67
Eu_N	13.8	17.8	50.6	20.2	10.9	19.3	13.4	9	13.7	16.3	25.1	14.4	50.9
Eu^*_N	14.8	19.5	32.5	34.5	10.7	38.5	32	36.5	38	46.5	37	41.5	35
Tb	0.66	0.7	1.31	1.31	0	1.17	1.26	1.25	1.29	1.86	2.48	1.7	1.37
Ho	0.89	1.37	1.65	1.85	1.42	1.96	1.28	1.33	1.52	0.72	1.79	1.48	0.39
Yb	2.2	2.81	4.47	4.84	3.88	5.72	4.59	4.98	6.59	21.67	4.17	5.02	5.1
Lu	0.35	0.44	0.12	0.8	0.59	0.85	0.67	0.78	0.95	0	0.58	0.77	0.81
ΣREE	50.49	77.91	137.67	142.36	263.84	212.62	149.26	203.71	191.02	230.67	120.39	229.68	201.47
Th	1.92	2.1	12.71	12.39	5.87	10.13	13.34	24.65	20.7	25.79	9.94	27.2	23.28
Hf	2.34	2.73	6.87	6.67	5.05	8.1	6.15	6.44	7.46	7.03	5.41	6.7	6.78
Ta	0.37	0.42	1.05	0.93	1.3	1.11	0.79	0.94	1.43	1.49	0.62	1.21	1.49
Ba	102.4	86.3	59.6	106.1	357.1	784	610.9	1270.5	497.7	3829.7	172.3	523.3	667.2
Sc	35.53	34.39	23.64	25.81	3.47	6.27	3.38	2.76	3.13	2.35	22.15	3.96	2.2
Co	45.3	42.8	16.77	16.66	0.99	1.23	1.19	0.66	0.63	0.78	9.89	0.57	0.75
Cr	149	137	6	3	3	2	3	1	2	5	1	2	5
Ni	87	72	2	1	4	2	3	5	1	2	4	2	3
V	246	304	59	57	7	12	3	5	2	3	29	5	5
Zr	111	125	251	276	172	378	233	196	282	215	230	197	203
Y	24	30	48	50	46	59	48	52	69	66	51	60	59
Sr	164	198	195	152	82	103	267	30	34	98	118	98	35
Rb	15	17	6	21	85	63	77	175	95	125	7	115	148
$(La/Yb)_N$	2.79	3.59	3.8	4.26	12.41	5.82	4.99	6.63	4.93	1.69	3.91	7.87	6.28
$(Yb)_N$	10.6	13.5	21.44	23.21	18.61	27.43	21.92	23.88	31.61	104.2	20	24.08	24.46

Table A3. Sunset Lake subarea.

Sample No.:	1	2	3	4	5	6	7	8	9	10	11
Field No.:	557	558	416	437	375	544	546	431	408	383	554
Volc. class:	Bs	Bs	Bs	Bs	Bs-An	Bs-An	An	An	An	An	An
La (ppm)	3.2	3.1	2.4	3.5	4.4	4.5	17.5	17.2	10.3	19.5	13.1
Ce	8.3	8.5	8.7	7.57	10	9.7	32.7	35.1	25	42.1	22.1
Nd	4.63	3.42	2.16	4.56	5.27	7.19	12.1	14.29	9.09	12.81	8.57
S_m	2.48	1.89	1.53	1.85	2.45	2.49	3.83	3.82	2.5	4.04	2.89
Eu	0.72	3.87	3.88	0.73	0.78	0.87	0.82	0.79	3.81	1.06	0.78
Eu_N	9.9	53.5	53.7	10.1	10.8	12.1	11.4	11	52.8	14.7	10.8
Eu_N	12.8	10	8	9.6	14.5	13.2	18.7	17.5	12.2	17.5	14.5
Tb	0.6	0.49	0.43	0.48	0.91	0.69	0.8	0.67	0.52	0.59	0.65
Ho	1.04	0.61	1.01	1.08	1.29	1.69	0.83	0.97	0.86	1.04	1.79
Yb	2.67	1.99	1.48	1.6	2.65	2.61	2.31	2.52	2.18	2.48	2.45
Lu	0.39	0.38	0.22	0.24	0.35	0.43	0.32	0.44	0.36	0.35	0.36
ΣREE	24.03	24.25	21.81	12.61	28.1	30.17	71.21	75.8	54.62	83.97	52.69
Th	0.15	0.21	3.87	0.62	0.9	0.84	4.06	4.22	3.05	5.66	5.06
Hf	2.23	1.37	1.22	0.98	2.53	1.66	3.16	3.89	3.26	3.51	1.94
Ta	0.21	0.11	0.14	0.09	0.13	0.13	0.44	0.44	0.45	0.57	0.29
Ba	0.1	71.6	344.9	9.8	0.1	42.6	190	154.2	413.9	320.4	58.5
Sc	40.96	40.9	43.69	35.23	50.15	44.4	22.12	24.02	25.73	26.15	20.28
Co	50.58	48.88	51.02	49.12	60.39	53.87	26.42	21.99	28.59	31.08	22.23
Cr	219	194	292	380		341	197	53	230	177	131
Ni	101	114	222	188	157	165	83	40	114	91	47
V	242	237	232	192	311	303	199	195	230	176	159
Zr	66	54	51	50	78	82	149	170	127	165	89
Y	26	21	15	20	29	28	25	28	20	27	24
Sr	106	140	73	189	136	139	120	139	62	202	120
Rb	2	3	20	3	3	5	17	13	26	15	6
$(La/Yb)_N$	0.79	1.03	1.07	1.44	1.1	1.14	5	4.51	3.12	5.19	3.53
$(Yb)_N$	12.81	9.54	7.12	7.67	12.7	12.52	11.08	12.06	10.5	11.9	11.75

12	13	14	15	16	17	18	19	20	21	22	23	24
545	541	410	543	556	398	552	535	534	562	413	412	384
An	An	An	Dc	Dc	Bs-An	Dc	Dc	Dc	Ry	Ry	Ry	Ry
27.5	54.5	19	21.7	15.9	24.7	21.4	16.3	22.8	60.1	51.7	48.8	34.7
58.2	115.9	36.8	50	34.1	53.9	39.4	31	43.7	128.3	130.7	102.4	74.3
15.78	51.9	12.57	16.21	14.96	26.52	16.88	10.08	15.78	45.67	44.13	34.04	25.32
4.72	9.09	3.58	5.04	3.7	8.2	4.33	3.28	4.7	11.39	9.66	8.18	5.61
3.99	3.86	0.62	4	0.96	1.9	0.89	0.99	1.21	0.62	3.86	0.73	0.65
55.2	53.5	8.6	55.3	13.4	26.3	12.3	13.8	16.7	8.6	53.4	10.1	9
21	37	17	20.5	16.5	38	19.5	18.3	20.5	46	43	34	26.5
0.74	1.11	0.71	0.64	0.59	1.52	0.79	1.03	0.71	1.99	1.54	1.09	1.08
0.4	0.97	0.3	1.05	0.64	1.71	1.1	2.13	0.86	2.14	1.18	0.59	0.98
2.73	3.8	2.57	2.38	1.14	6.84	2.7	1.85	2.43	6.4	4.72	3.34	3.66
0.4	0.54	0.39	0.36	0.22	1.06	0.45	0.26	0.35	0.97	0.68	0.5	0.6
114.46	241.67	76.54	101.38	72.21	126.35	87.94	66.92	92.54	257.58	248.17	199.67	146.9
9.97	5.41	9.79	5.56	1.16	6.29	4.58	0.58	5.44	24.98	26.32	20.52	18.61
4.42	6.39	3.52	4.73	3.62	5.78	3.25	2.84	3.64	6.51	7.58	5.57	4.04
0.56	1.06	0.46	0.79	0.49	0.89	0.42	0.33	0.5	1.04	1.54	0.8	0.73
395.2	546.1	142.1	190.7	211.3	344.1	208	160.5	70.7	812.4	461.8	40.7	796.6
18.81	15.74	17.57	18.73	8.37	46.93	20.29	16.42	16.25	6.32	3.17	1.89	2.38
20.88	23.61	20.12	16.06	11.22	50.3	25.31	16.34	18.58	2	1.73	1.03	0.89
20	25	100	44	21	46	98	74	43	1	3	1	2
9	14	33	33	10	25	53	36	26	2	11	1	1
227	130	128	152	78	396	211	140	137	2	5	3	2
191	290	122	205	195	211	187	147	189	200	217	176	125
31	41	25	29	16	61	28	23	27	71	51	37	38
240	223	106	289	312	131	183	211	283	51	82	76	43
33	36	23	13	14	93	21	24	9	122	77	24	70
6.65	9.47	4.88	6.02	9.21	2.38	5.23	5.82	6.2	6.2	7.23	9.65	6.26
13.09	18.22	12.4	11.41	5.47	32.9	12.95	8.87	11.65	30.69	22.7	16.1	17.6